Research Square

Preprints are preliminary reports that have not undergone peer review.
They should not be considered conclusive, used to inform clinical practice,
or referenced by the media as validated information.

Clumped isotope thermometry determines diagenetic origin of the crystalline dolomite

Jiakai Hou

geohjk@163.com

Research Institute of Petroleum Exploration and Development

Guangyou Zhu

Yangtze University

Hongbin Li

China University of Petroleum (Beijing)

Lizhen Wang

Research Institute of Petroleum Exploration and Development

Article

Keywords: Crystalline dolomite, Clumped isotope, Dolomitization, Xixiangchi formation, Sichuan basin

Posted Date: August 14th, 2025

DOI: https://doi.org/10.21203/rs.3.rs-7244432/v1

License: This work is licensed under a Creative Commons Attribution 4.0 International License.
Read Full License

Additional Declarations: No competing interests reported.

Clumped isotope thermometry determines diagenetic origin of the crystalline dolomite

Jiakai Hou [a, *], Guangyou Zhu [b, *], Hongbin Li [c], Lizhen Wang [a]

[a] Research Institute of Petroleum Exploration and Development, PetroChina, Beijing 10083, China

[b] School of Geoscience, Yangtze University, Wuhan 430100, China

[c] College of Geosciences, China University of Petroleum (Beijing), Beijing 102249, China

***Corresponding author:** (Jiakai Hou). Tel.: +86 15694823661*
E-mail address: geohjk@163.com

*** Co-Corresponding author:** (Guangyou Zhu). Tel.: +86 18601309981*
E-mail address: zhuguangyou@yangtzeu.edu.cn

Abstract: The origin of widespread crystalline dolomite deposits in the Cambrian strata of southwestern China is a longstanding open question. Here, we use a suite of petrology and geochemical methods to investigate the occurrence of crystalline dolomites in the Middle-Upper Cambrian Xixiangchi Formation within the Sichuan Basin. Four texturally distinct dolomite types (D1-D4) were identified, spanning micritic to medium crystalline morphologies. Clumped isotope measurements can potentially provide better constraints for the origin of crystalline dolomite. Still, most of the Cambrian crystalline dolomites experienced burial temperatures above the limits of preservation of Δ_{47}. Prior bond reordering kinetics models predicted that dolomite Δ_{47} values could be preserved at ambient temperatures lower than 120-150 ℃ for tens of million years. However, before being uplifted to the current depth of 4.5-5.5 km, the dolomites of the Xixiangchi Formation experienced high temperature up to 230 ℃ during the late deep burial process. Samples from the Sichuan basin are expected to be partially reordered and yield significant Δ_{47} fractionation. The Δ_{47} evolution of the crystalline dolomites was predicted with the exchange/diffusion model under the constraints of independent thermal history reconstruction and Δ_{47} values. By integrating the corrected $\delta^{18}O_{fluid}$-$T_{\Delta47}$ data, trace element composition, C-O-Sr isotope data, and crystal structure characteristics of dolomite, we propose that the dolomitization fluid of Xixiangchi Formation is mainly the contemporaneous seawater of the Cambrian, with crystal ordering evolution controlled by burial temperature and fluid-rock interaction dynamics.

Keywords: Crystalline dolomite; Clumped isotope; Dolomitization; Xixiangchi formation; Sichuan basin

Introduction

Since the discovery of dolomite [$CaMg(CO_3)_2$] in 1791, its formation mechanism has garnered significant attention from geologists. Theoretically, modern seawater is supersaturated with respect to dolomite[1], with a Mg/Ca ratio of approximately 5.2, which should facilitate large-scale dolomitization. However, the precipitated carbonate mineral is typically aragonite instead. Previous attempts to synthesize dolomite in laboratory settings under surface

conditions (ambient temperature and pressure) have failed[2], further complicating the "dolomite problem".

In carbonate reservoirs, crystalline dolomite is an important reservoir rock type due to its well-developed intercrystalline porosity, which imparts excellent reservoir properties. The protolith of crystalline dolomite is predominantly grainstone, and as burial depth increases and dolomitization persists, the crystal size of dolomite progressively enlarges[3]. When the size of dolomite crystals surpasses that of the original grains, the texture of the protolith becomes difficult to preserve, and the associated geochemical signals are likely to be altered by subsequent recrystallization. Crystalline dolomite is widely distributed in the Sichuan Basin, Tarim Basin, and Ordos Basin of China[4]. Previous studies have proposed several hypotheses regarding the formation mechanism of crystalline dolomite. Penecontemporaneous dolomitization has been suggested to transform limestones deposited in tidal flat environments into fine to medium crystalline dolomite, with well-developed intercrystalline porosity developing during this process[5]. In contrast, mixed-water dolomitization has been argued as the primary controlling factor for the formation of crystalline dolomite with good reservoir properties[6], while contemporaneous meteoric water leaching has been proposed as key to the formation of large-scale crystalline dolomite[7]. Given these contradictory mechanisms, the genetic origin of crystalline dolomite remains inconclusive and warrants further investigation.

In reality, dolomitization is a complex, multi-stage process involving various geological conditions and time periods[8]. As such, the formation of dolomite is typically influenced by a combination of factors, including fluid chemistry, thermodynamics, and kinetics[9]. It is challenging to fully explain the genesis of dolomite using a single dolomitization model or research method. There are diverse approaches to studying dolomite formation, and the trace elements and C, O, and Sr isotopes in dolomites can help identify the types of diagenetic fluids involved in diagenetic events and associate these events with specific diagenetic environments[10, 11].

In recent years, the rapid development of unconventional research methods, such as the study of dolomite crystal structure and clumped isotopes, has further advanced our understanding of dolomitization processes and their evolutionary mechanisms. The crystal structure, degree of order, and unit cell parameters of dolomite reflect characteristics related to crystallization, growth, and nucleation during dolomite formation[12]. These factors serve as key indicators for investigating the stages of dolomite formation and the sequence of diagenesis. When studying the temperature of dolomite formation and the properties of dolomitizing fluids, traditional oxygen isotope thermometry, used to determine carbonate rock temperatures, can be influenced by the oxygen isotopic composition of the parental fluid[13], leading to ambiguities in determining the diagenetic temperature of the mineral. Moreover, modern formation waters in dolomite reservoirs have often undergone complex hydrocarbon-water-rock interactions after dolomitization[14], making it difficult to represent the fluid properties from the time of dolomitization accurately. In contrast, carbonate clumped isotopes (Δ_{47}) allow for the direct determination of the formation temperature of carbonate minerals, such as calcite or dolomite[15]. By combining this with the $\delta^{18}O$ of the mineral itself, the $\delta^{18}O$ of the parental fluid can be calculated, providing a novel solution for determining the $\delta^{18}O$ of dolomitizing fluids[16]. Currently, Δ_{47} has been widely applied to investigate the sources and models of dolomitizing fluids[17, 18]. However, during deep burial, dolomites are subject to high-temperature solid-state reordering[3], which can alter the Δ_{47}[19]. This introduces certain limitations when using Δ_{47} to determine the $\delta^{18}O$ of dolomitizing fluids[20]. Thus, further simulations are needed to restore the Δ_{47} values from the diagenetic period.

In the carbonate gas fields of the Sichuan Basin, over 90% of natural gas reserves are concentrated in dolomite

reservoirs within the Sinian, Cambrian, Carboniferous, Permian, and Triassic systems[4]. The Middle-Upper Cambrian Xixiangchi (XXC) Formation is a key exploration target and successor to the current productive horizons in the Sichuan Basin. The XXC Formation is composed of thick dolomites, especially crystalline dolomite, and the thickness can reach 600 m in some areas[21]. In comparison to the thick-bedded beach facies dolomite reservoirs of the Longwangmiao Formation, the crystalline dolomite reservoirs of the XXC Formation are thinner vertically, have limited lateral distribution, and exhibit strong heterogeneity[22], and the genesis mechanism of crystalline dolomite remains unclear. To further address the "dolomite problem," this study focuses on the crystalline dolomites of the XXC Formation, specifically from the GT2 well, which provides continuous core samples in the Sichuan Basin. Through a comprehensive investigation involving petrography, X-ray diffraction (XRD) analysis, trace elements, Sr isotopes, clumped isotopes, and C and O isotope analyses, this study uncovers the response of dolomite crystal structures to depositional environments. It also reconstructs the initial diagenetic temperatures of different types of crystalline dolomites and identifies the characteristics of diagenetic fluids and the dolomitization mechanisms in the XXC Formation. The findings provide a robust foundation and scientific basis for future petroleum exploration and development of dolomite reservoirs in the Middle-Upper Cambrian XXC Formation in the Sichuan Basin.

Geological setting

The Cambrian South China Craton lies to the northwest of the supercontinent Gondwana (Fig. 1a). During the convergence of the Gondwana supercontinent, the Gondwana supercontinent converged in the southern hemisphere (Fig. 1a), and the South China block obviously drifted southward during the Cambrian Period[23]. The jointing force of ocean-land distribution and the orbital obliquity of the Earth caused the intertropical convergence zone (ITCZ) of the Hadley Cell to shift northward during the Cambrian Terreneuvian and Series 2 periods[24]. Consequently, as the South China block drifted southward through the humid, transitional and arid belts, organic-rich shales, carbonates, and evaporites were deposited[25].

The Sichuan Basin, located in the northwest of the Yangtze Block in China (Fig. 1b), is surrounded by the Micang, Daba, Qiyue, and Longmen mountains (Fig. 1c). It is a large, multi-cycle superimposed petroleum basin, structurally controlled by deformation in its surrounding orogenic belts[26]. During the Cambrian period, the Sichuan Basin was a stable craton basin, characterized by a west-high, east-low depositional pattern[24]. The study area is mainly located in the Gaoshiti-Moxi paleo-uplift in the central Sichuan Basin, where the Cambrian strata, from bottom to top, comprise the Lower Cambrian Qiongzhusi, Canglangpu, and Longwangmiao Formations, the Middle Cambrian Gaotai Formation, and the Middle-Upper Cambrian XXC Formation (Fig. 1d).

During the depositional period of the Lower Cambrian Longwangmiao Formation, a ramp depositional model developed in an evaporative environment[27], indicating a regression and salinization of seawater. In the Middle Cambrian Gaotai Formation, the basin retained its northwest-high, southeast-low depositional pattern[28], with continued regression and the expansion of the paleo-continent. The Middle-Upper Cambrian XXC Formation preserved the northwest-high, southeast-low paleogeographic pattern, with an evaporative salt basin developing in the central part of the basin[29]. During the early stages of deposition, a rapid, large-scale marine transgression occurred, covering much of the Sichuan Basin with restricted platform facies. Controlled by paleogeography, high-

energy grain shoals developed on both sides of the platform depression, where water energy was relatively higher[30]. Overall, the XXC Formation in the study area represents a transgressive-regressive depositional cycle, dominated by restricted platform facies. The dolomites of the XXC Formation are lithologically uniform, consisting mainly of crystalline dolomite. The formation thickness increases from west to east, reaching up to 700 m in some areas, and exhibits a depositional pattern of land in the west and sea in the east[8].

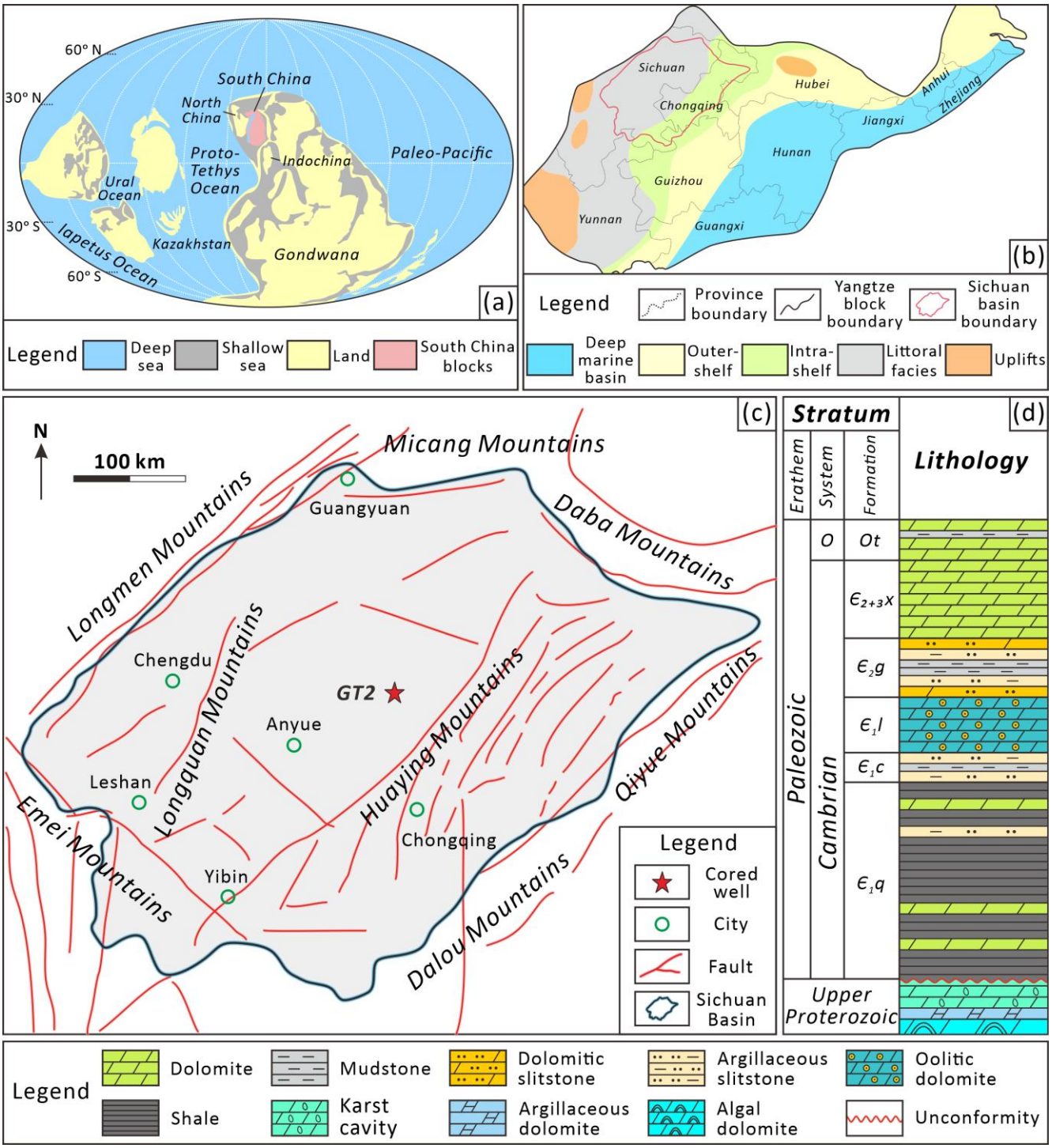


Figure 1. (a) Cambrian palaeogeographic maps (modified after[24]); (b) Sedimentary facies map of the Yangtze Block (modified after[31]); Structural map of the Sichuan Basin showing (c) the location of the cored well and (d) the general

stratigraphic framework of the investigated Middle-Upper Cambrian XXC Formation (modified after[29]). Notes: ϵ_1q, the Lower Cambrian Qiongzhusi Formation; ϵ_1c, the Lower Cambrian Canglangpu Formation; ϵ_1l, the Lower Cambrian Longwangmiao Formation; ϵ_2g, the Middle Cambrian Gaotai Formation; $\epsilon_{2\text{-}3}$x, the Middle-Upper Cambrian Xixiangchi Formation; O_t, the Ordovician Tongzi Formation.

Samples and methods

Petrological analyses

In the laboratory, the collected samples were prepared as polished sections with a thickness of 0.5 mm, along with corresponding petrographic thin sections. These were then examined using a Nikon Eclipse LV100N POL optical microscope to identify the mineral composition, crystal structures, and pore types present in the rock samples.

X-ray diffraction (XRD) was employed to analyze the mineral composition, degree of ordering, and cell parameters of the dolomites. This analysis was conducted at the Key Laboratory of the Institute of Mineral Resources, Chinese Academy of Geological Sciences. The instrument used was a PANalytical X-ray diffractometer, operating at a voltage of 40 kV and a current of 40 mA, with a scanning range of 4-60° 2θ.

Trace element analysis

Trace element analysis was performed using an inductively coupled plasma optical emission spectrometer (ICP-OES) at the ICP Spectroscopy Laboratory of the School of Earth and Space Sciences, Peking University. A 50 mg powdered dolomite sample was placed into a 15 mL test tube, followed by the addition of 5 mL of 5 N acetic acid to dissolve the powder. The test tube was then subjected to an ultrasonic bath for 30 minutes, after which it was centrifuged at 3000 rpm for 10 minutes. The supernatant was collected for trace element composition analysis.

Isotope analyses

Nine powdered samples were selected for clumped isotope analysis at the China University of Geosciences at Wuhan using the same conditions (e.g., 90 °C acid reaction temperature) reported by[15]. In establishing the absolute reference frame (ARF), tests were conducted using high-temperature gases at 1000°C, along with equilibrium gases at 10°C, 25°C, and 50°C. Standard carbon and oxygen isotopes ($\delta^{13}C$ and $\delta^{18}O$) were also acquired in this process. The analysis of carbonate clumped isotope data was automatically performed using the Easotope software, and the clumped isotope calculation followed the formula provided by[32]:

$$\Delta_{47} = \left[\left(\frac{R^{47}}{R^{47*}} - 1\right) - \left(\frac{R^{46}}{R^{46*}} - 1\right) - \left(\frac{R^{45}}{R^{45*}} - 1\right)\right] \times 1000 \qquad (1)$$

In Eq. (1), R^{45}、R^{46}、R^{47} represent the abundance ratios of isotopologues with masses 45, 46, and 47, respectively, relative to those with mass 44 in the CO_2. R^{45*}, R^{46*}, and R^{47*} denote the abundance ratios of these isotopologues after being heated at 1000°C for 2 hours, reaching a state of random distribution.

The use of Δ_{47} to determine the formation temperature of carbonate minerals such as calcite and dolomite is referred to as the clumped isotope thermometer[33]. The clumped isotope thermometer is based on the exchange reaction of ^{13}C and ^{18}O (Eq. 2)[34]. The abundance of ^{13}C-^{18}O bonds is a function of the equilibrium constant of this reaction, which is temperature-dependent and is influenced only by temperature. Various empirical formulas have been established by previous researchers to describe the relationship between Δ_{47} and $T_{\Delta47}$, the Δ_{47}-T calibrations recommended by Bonifacie[35] (Eq. 3) and by Müller[36] (Eq. 4) for dolomite and Petersen[37] (Eq. 5) and Anderson[38] (Eq. 6) for carbonate minerals are used to constrain the relationship between dolomite formation temperature (T) and clumped isotope values (Δ_{47}):

$$Ca^{13}C^{16}O_3 + Ca^{12}C^{18}O^{16}O_2 = Ca^{13}C^{18}O^{16}O_2 + Ca^{12}C^{16}O_3 \quad (2)$$

$$\Delta_{47CDES90} = 0.0428 * (10^6 / T^2) + 0.1174 \ (r^2 = 0.997) \ (90°C \text{ acid reaction temperature}) \quad (3)$$

$$\Delta_{47CDES70} = 0.0428 * (10^6 / T^2) + 0.1481 \ (r^2 = 0.864) \ (70°C \text{ acid reaction temperature}) \quad (4)$$

$$\Delta_{47CDES25} = 0.0383 * (10^6 / T^2) + 0.258 \ (r^2 = 0.864) \ (25°C \text{ acid reaction temperature}) \quad (5)$$

$$\Delta_{47(I\text{-}CDES90)} = 0.0390 * (10^6 / T^2) + 0.153 \ (r^2 = 0.970) \ (90°C \text{ acid reaction temperature}) \quad (6)$$

In Eq. (3), (4), (5), (6), Δ_{47} represents the value measured under different temperature conditions, corrected for acid digestion, ‰; T refers to the equilibrium temperature of dolomite formation. Typically, carbonate mineral powder samples for clumped isotope analysis are digested in acid at 25°C. However, under such low-temperature conditions, the reaction rate is slow, and testing a single sample can take 10-12 hours. In this experiment, the powdered dolomite samples were instead digested at 90°C, and the clumped isotope data at 90 °C acid digestion were standardized using the ARF as suggested by Dennis[32]. The $T_{\Delta47}$ was calculated using the empirical relationships provided in Eq. (3) and (6) (Fig. 2).

Sr isotope analysis was conducted at the Key Laboratory of the Institute of Mineral Resources, Chinese Academy of Geological Sciences. For each analysis, 50 mg of powdered sample was dissolved in a Teflon cup at 190°C for 15 hours using twice-distilled HNO_3, HCl, and HF. Sr was purified using Sr-spec resin columns, with approximately 500 ng of Sr isolated from each sample for isotope measurement. Sr isotope ratios were determined using a NuPlasmaII multi-collector inductively coupled plasma mass spectrometer (MC-ICP-MS), with NIST-987 used as the reference standard.

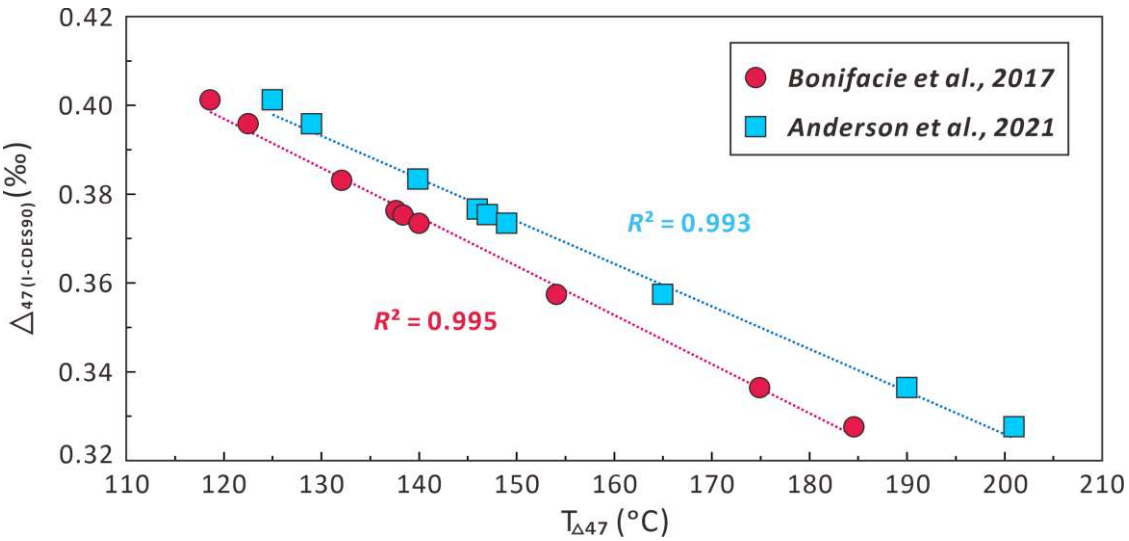


Figure 2. Δ_{47} versus $T_{\Delta47}$. Based on the Δ_{47}-T calibrations established by[35] and[38].

Results

Structural types and characteristics of dolomite

The Middle-Upper Cambrian XXC Formation dolomites in the study area predominantly consist of crystalline dolomites where the original depositional structures are difficult to identify. These include micrite dolomite (D1), powder crystalline dolomite (D2), finely crystalline dolomite (D3), and medium crystalline dolomite (D4). Given that crystalline dolomites often exhibit variations in crystal morphology, particularly at the "fine crystalline" level, where crystals of similar size may exhibit vastly different shapes, this study incorporates the terms "euhedral," "subhedral," and "anhedral" as proposed by Sibley[39] to distinguish the differences in crystal structure.

Micrite dolomite (D1)

Micrite dolomite is characterized by its dense lithology (Fig. 3a-c), primarily composed of anhedral micritic dolostones. These crystals are extremely small, with diameters ranging from 10 to 30 μm, averaging 15 μm. The crystals are tightly packed, with minimal development of intercrystalline pores or dissolution pores. Gypsum and argillaceous bands, commonly associated with micrite dolomites, can be observed in the core samples.

Powder crystalline dolomite (D2)

Powder crystalline dolomite is predominantly composed of subhedral to anhedral powder dolostones (Fig. 3d-f), with crystal sizes ranging from 50 to 100 μm, averaging 60 μm. The crystals exhibit a mosaic or linear contact pattern, with slightly dirty surfaces and irregular bright edges. Intercrystalline pores are poorly developed.

Finely crystalline dolomite (D3)

Finely crystalline dolomite is dominated by subhedral to euhedral dolostones (Fig. 3g-i), with crystal diameters ranging from 80 to 250 μm, averaging 150 μm. The crystals are relatively clean with well-formed, straight boundaries, predominantly exhibiting point or line contact. This type of dolomite has a porous "sucrosic" texture, though most of the intercrystalline pores are filled with organic matter or calcite, and some euhedral dolostone rhombohedra display well-developed zoning.

Medium crystalline dolomite (D4)

Medium crystalline dolomite consists of subhedral to anhedral dolostones (Fig. 3j-l), with crystal diameters ranging from 250 to 500 μm, averaging 300 μm. In some medium crystalline dolomites, intercrystalline and dissolution pores are well-developed and often filled with solid bitumen (Fig. 3j, l), indicating that these pores served as the primary reservoir space in ancient petroleum systems. The crystal surfaces are typically dirty, often displaying a "cloudy core and bright rim" texture (Fig. 3k). Subhedral crystals are typically scattered (Fig. 3j, l), while anhedral crystals tend to form clusters or aggregates with irregular contacts (Fig. 3k). A few medium crystalline dolomite grains exhibit relic grain structures, although recrystallization has largely obliterated the original depositional

characteristics, indicating that these medium crystalline dolomites are the result of multiple stages of metasomatism or recrystallization in a burial environment.

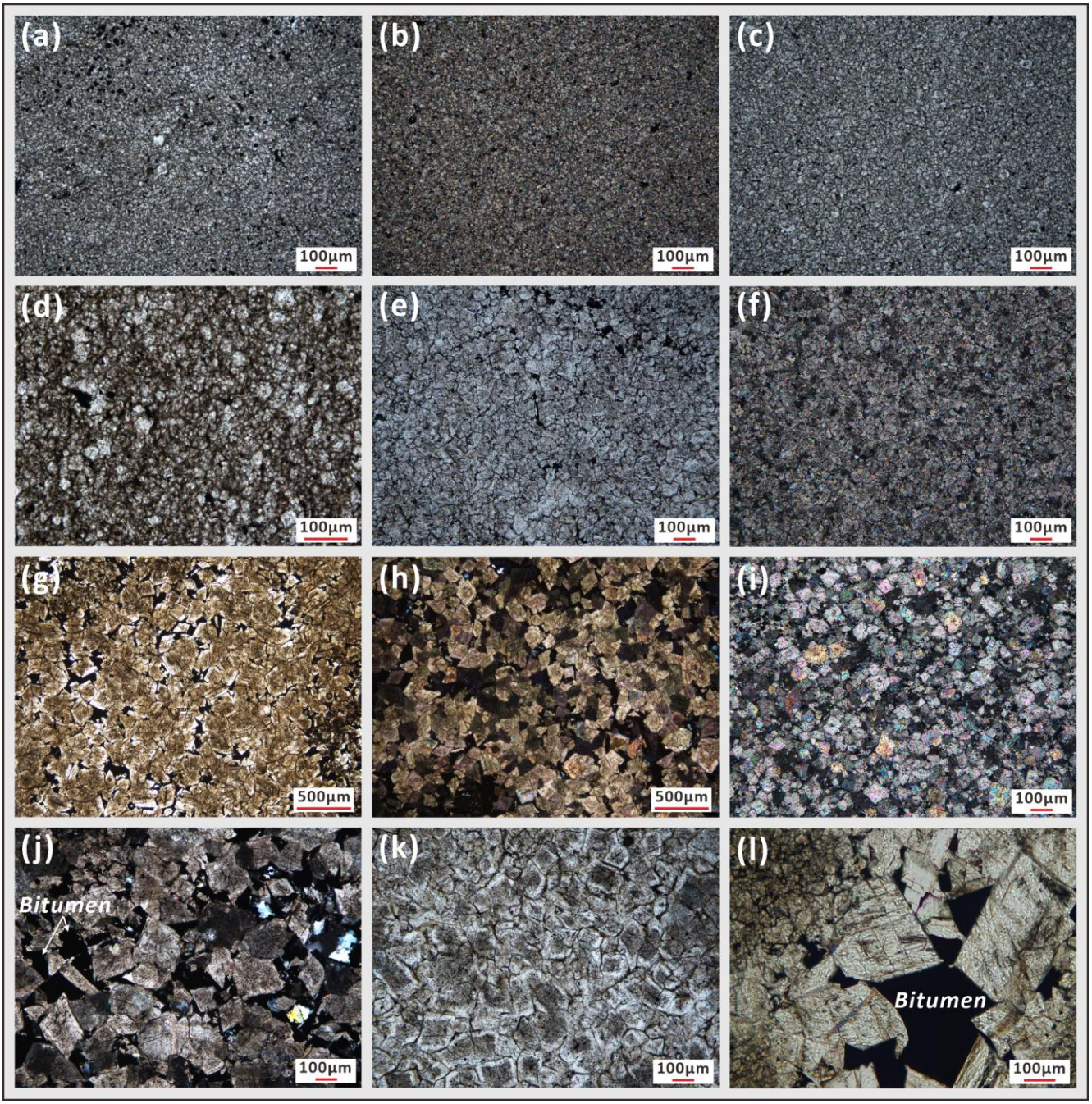


Figure 3. Photomicrographs of the main petrographic characteristics of the Middle-Upper Cambrian XXC Formation dolomites. (a-c) Micrite dolomite (D1) from well GT2, 5338.8-5339.4 m; (d-f) Powder crystalline dolomite (D2) from well GT2, 5333.4-5333.8 m; (g-i) Fine crystalline dolomite (D3) from well GT2, 5340.4-5340.9 m; (j-l) Medium crystalline dolomite (D4) from well GT2, 5345.0-5346.7 m.

XRD and unit cell parameters

XRD analysis can be used to determine the unit cell parameters and ordering of dolomite crystals. Well-ordered

dolomite exhibits superstructure reflections, which are particularly evident at the (015) and (110) diffraction peaks. Füchtbauer proposed using the ratio $I_{(015)}/I_{(110)}$ to calculate the degree of dolomite ordering[40]. When Mg^{2+} and Ca^{2+} alternate along the (001) plane, $I_{(015)}/I_{(110)} = 1$, while a completely disordered arrangement yields $I_{(015)}/I_{(110)} = 0$. Based on this method, XRD analysis and data processing were conducted on the crystalline dolomites from the XXC Formation (Table 1). D1 exhibited a relatively low degree of ordering, with values ranging from 0.67 to 0.80 (average of 0.74). Its unit cell parameters ranged from 4.796 Å to 4.803 Å for a and from 15.977 Å to 16.004 Å for c. D2 showed an ordering degree ranging from 0.65 to 0.83 (average of 0.74). The unit cell parameter a ranged from 4.795 Å to 4.804 Å, and the unit cell parameter c from 15.977 Å to 16.001 Å. D3 exhibited a higher degree of ordering compared to D1 and D2, ranging from 0.69 to 1.02 (average of 0.84), with the unit cell parameter a between 4.799 Å and 4.806 Å, and the unit cell parameter c between 15.976 Å and 16.007 Å. D4 had the highest degree of ordering, ranging from 0.80 to 1.06 (average of 0.86). The unit cell parameter a ranged from 4.799 Å to 4.806 Å, while the unit cell parameter c spanned from 15.983 Å to 16.011 Å.

Table 1 Summary statistics of unit cell parameters, isotopic data, and elemental concentrations of D1, D2, D3, and D4 in the XXC Formation.

Dolomite type		$N(MgCO_3)$ (%)	50-$N(MgCO_3)$ (%)	Unit cell parameter a (Å)	Unit cell parameter c (Å)	a/c	Degree of ordering	Mg/Ca	Mn/Sr	$^{87}Sr/^{86}Sr$
D1	n	8	8	8	8	8	8	7	7	7
	Mean	49.18	1.14	4.800	15.990	0.30018	0.74	1.01	1.89	0.70956
	S.D.	0.85	0.28	0.002	0.008	0.00004	0.04	0.02	1.20	0.00040
	Max	51.30	1.63	4.803	16.004	0.30024	0.80	1.05	4.14	0.71043
	Min	48.37	0.7	4.796	15.977	0.30012	0.67	0.99	0.77	0.70929
D2	n	11	11	11	11	11	11	11	11	11
	Mean	49.12	0.99	4.800	15.990	0.30019	0.74	1.00	1.91	0.70987
	S.D.	0.62	0.43	0.003	0.007	0.00006	0.06	0.02	1.16	0.00043
	Max	50.57	1.77	4.804	16.001	0.30026	0.83	1.03	4.28	0.71066
	Min	48.23	0.33	4.795	15.977	0.30010	0.65	0.98	0.42	0.70926
D3	n	22	22	22	22	22	22	22	22	20
	Mean	49.56	0.66	4.802	15.996	0.30022	0.84	1.00	1.42	0.71015
	S.D.	0.65	0.43	0.002	0.007	0.00008	0.07	0.01	0.66	0.00042
	Max	51.87	1.87	4.806	16.007	0.30037	1.02	1.02	3.40	0.71095
	Min	48.40	0.03	4.799	15.976	0.30007	0.69	0.99	0.64	0.70941
D4	n	8	8	8	8	8	8	8	8	8
	Mean	49.66	0.34	4.804	16.001	0.30023	0.86	1.01	1.38	0.71026
	S.D.	0.19	0.19	0.003	0.009	0.00004	0.08	0.01	0.47	0.00021
	Max	50.00	0.63	4.806	16.011	0.30029	1.06	1.03	2.28	0.71055
	Min	49.37	0.17	4.799	15.983	0.30018	0.80	1.00	0.71	0.70990

Characteristics of trace elements

In Table 1, geochemical results of trace elements in crystalline dolomite of XXC Formation in the study area are presented. D1 exhibited relatively high Mn/Sr ratios, ranging from 0.77 to 4.14 with an average of 1.89. The Mg/Ca values ranged between 0.99 and 1.05, averaging 1.01. D2 had a wide range of Mn/Sr values, from 0.42 to 4.28 with an average of 1.91. Its Mg/Ca values ranged between 0.98 and 1.03, averaging 1.00. D3 showed Mn/Sr ratios between 0.64 and 3.40, with an average of 1.42. The Mg/Ca values ranged from 0.99 to 1.02, with an average of 1.00. D4 displayed Mn/Sr ratios ranging from 0.71 to 2.28, with an average of 1.38. Its Mg/Ca values were close to 1, ranging from 1.00 to 1.03 with an average of 1.01.

$^{87}Sr/^{86}Sr$ ratios

By analyzing the $^{87}Sr/^{86}Sr$ ratios of different types of crystalline dolomites in the XXC Formation (Table 1), this study investigates the geochemical conditions and fluid sources associated with dolomite formation. The results reveal varying $^{87}Sr/^{86}Sr$ values across the different structural types: D1 exhibits $^{87}Sr/^{86}Sr$ values ranging from 0.70929 to 0.71043, with the smallest average value of 0.70956. D2 has $^{87}Sr/^{86}Sr$ values between 0.70926 and 0.71066, with an average of 0.70987. D3 shows the largest range, with values from 0.70941 to 0.71095, averaging 0.71015. D4 has $^{87}Sr/^{86}Sr$ values ranging from 0.70990 to 0.71055, with an average of 0.71026.

^{13}C, ^{18}O, Δ_{47} and $T_{\Delta 47}$

In this study, stable isotopes and clumped isotopes of nine crystalline dolomite samples from the Cambrian XXC Formation were analyzed (Table 2). The $\delta^{13}C$ values of all samples range from -4.31‰ to -1.07‰, with an average of -2.34‰, while $\delta^{18}O$ values range from -6.38‰ to -5.27‰, with an average of -5.92‰. The isotopic composition varies significantly across different structural types of dolomites: D1 has $\delta^{13}C$ values ranging from -2.94‰ to -2.86‰ (average -2.90‰) and $\delta^{18}O$ from -5.79‰ to -5.27‰ (average -5.53‰). D2 exhibits $\delta^{13}C$ values between -1.98‰ and -1.26‰ (average -1.62‰) and $\delta^{18}O$ values from -6.38‰ to -6.01‰ (average -6.20‰). D3 shows a broader range of $\delta^{13}C$ from -4.31‰ to -1.07‰ (average -2.84‰) and $\delta^{18}O$ from -6.18‰ to -5.41‰ (average -5.92‰). D4 has $\delta^{13}C$ values between -1.76‰ and -1.71‰ (average -1.74‰) and $\delta^{18}O$ from -6.13‰ to -5.99‰ (average -6.06‰). After calibrating to the ARF using the Δ_{47}-T calibration from Bonifacie[35], the calculated temperatures derived from the clumped isotopes ($T_{\Delta 47}$) range from 118.6 °C to 184.6 °C, with an average of 144.8 °C (Table 2). Each $T_{\Delta 47}$ is similar to, or 6-16 °C lower than, the temperature derived by Δ_{47} using the calibration of Anderson[38] (Table 2).

Table 2 Composite temperature or diagenesis related geochemical data of dolomites from the XXC Formation.

Dolomite type	Δ_{47} (‰)	STF-$\Delta_{47ARF90}$ (‰)	$T_{\Delta47}$ [a] (℃)	$T_{\Delta47}$ [b] (℃)	Current $T_{\Delta47}$ (℃) by SE-Model	Initial $T_{\Delta47}$ (℃) by SE-Model	Diagenetic time (Ma)	$\delta^{13}C_{carb}$ (VPDB, ‰)	$\delta^{18}O_{carb}$ (VPDB, ‰)	Z	$\delta^{18}O_{fluid}$ [c] (VSMOW, ‰)	$\delta^{18}O_{fluid}$ [d] (VSMOW, ‰)
D1	0.400	0.4012	125	118.6	110.9	25.9	518.8	-2.94	-5.79	118.4	13.92	-0.82
	0.395	0.3958	129	122.5	123.9	28.7	516.4	-2.86	-5.27	118.8	14.86	0.35
D2	0.376	0.3762	146	137.7	137.9	52.8	510.4	-1.26	-6.38	121.5	15.22	4.16
	0.374	0.3734	149	140.0	142.9	63.4	503.9	-1.98	-6.01	120.3	15.80	6.37
D3	0.383	0.3831	140	132.1	136.1	51.5	510.9	-4.31	-5.41	115.8	15.67	4.89
	0.375	0.3753	147	138.4	140.4	60.1	504.6	-1.07	-6.18	122.0	15.48	5.64
	0.359	0.3574	165	154.1	146.1	73.3	475.4	-3.14	-6.16	117.8	16.86	7.79
D4	0.339	0.3364	190	174.9	174.4	110.5	251.8	-1.76	-5.99	120.7	18.62	12.84
	0.331	0.3276	201	184.6	178.2	116.2	247.5	-1.71	-6.13	120.7	19.15	13.29

[a] The $T_{\Delta47}$ values were calculated using the calcite temperature calibration in Anderson[38].

[b] The $T_{\Delta47}$ values were calculated using the dolomite temperature calibration in Bonifacie[35].

[c] The $\delta^{18}O_{fluid}$ (VSMOW, ‰) value was calculated using the $T_{\Delta47}$ value which was calculated by using the revised dolomite temperature calibration in this study.

[d] The $\delta^{18}O_{fluid}$ (VSMOW, ‰) value was calculated using the initial $T_{\Delta47}$ value from modeling which is based on SE-Model.

Discussion

Dolomite crystal structure in response to the environment

The molar percentage of $MgCO_3$ in the dolomite

Dolomite can be categorized into ideal dolomite, where the Mg/Ca ratio is equal to the stoichiometric ratio, and non-ideal dolomite, where the Mg/Ca ratio deviates from this ideal ratio. In the structure of ideal dolomite, alternating layers of Mg^{2+} and Ca^{2+} ions are interspersed with CO_3^{2-} groups aligned perpendicular to the c-axis[12]. The molar fractions of Mg^{2+} and Ca^{2+} are equal, and Mg^{2+}, Ca^{2+}, and CO_3^{2-} ions are completely ordered in the crystal lattice (Fig. 4a). Due to the difference in ionic radii between Mg^{2+} and Ca^{2+}, changes in their content lead to alterations in the unit cell parameters. This is reflected in XRD patterns, where the position of the (104) diffraction peak shifts accordingly as the content of Mg^{2+} or Ca^{2+} changes (Fig. 4b). From a geochemical perspective, Zeng[41] derived an equation to calculate the molar fraction of $MgCO_3$:

$$N_{MgCO_3} = -333.33 d_{(104)} + 1011.99 \quad (7)$$

In Eq. (7), N represents the molar fraction content, %; $d_{(104)}$ is the interplanar spacing of the (104) plane, which can be calculated from the 2θ value of the diffraction peak in XRD patterns.

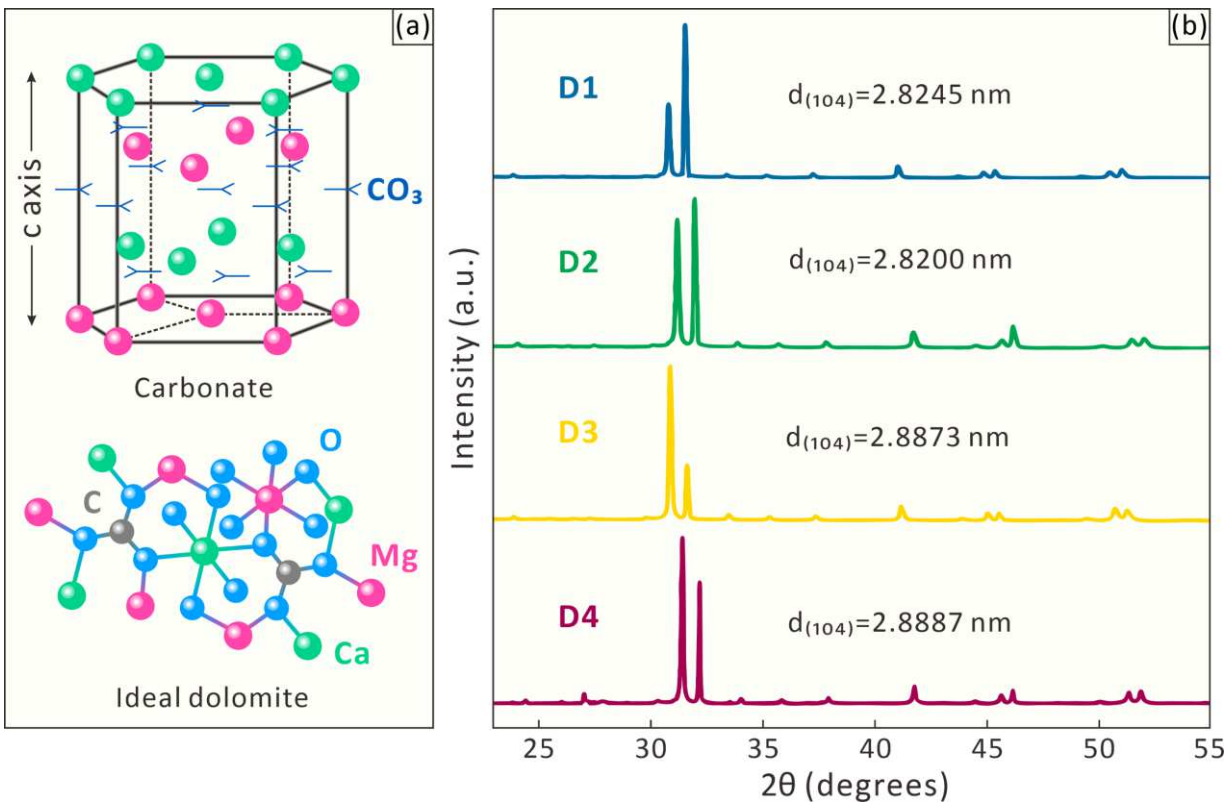


Figure 4. Crystal structure analysis of dolomite. (a) The ideal dolomite structure model was modified after[11, 43]; (b) Schematic calculation of the dolomite ordering degree based on XRD.

The molar fraction of $MgCO_3$ in the dolomite lattice is closely related to the ordering degree of dolomite[12]. A higher degree of order indicates that the molar fraction of $MgCO_3$ in the dolomite structure is closer to the theoretical

value of 50%. Previous studies have shown that ideal dolomite has a $CaCO_3/MgCO_3$ ratio of 50/50, while natural dolomites exhibit ratios ranging from 58/42 to 48/52[42]. Based on the XRD patterns of dolomite ordering (Fig. 4), the molar fractions of $MgCO_3$ in the dolomites from the study area were calculated. The majority of $MgCO_3$ molar fractions fall within the range of 48.0% to 51.5% (Fig. 5a), with the larger crystalline dolomites D3 and D4 exhibiting significantly higher degrees of ordering compared to D1 and D2. When the molar fraction of $MgCO_3$ is in the range of 49.3% to 50.5%, the ordering degree of the dolomites reaches its peak (Fig. 5b). This suggests that when the values of Mg^{2+} and Ca^{2+} in dolomite approach equilibrium, the likelihood of regular interlayer alternation of these ions increases substantially.

Since the ordering degree of dolomite is linked to its crystallization rate, the molar fraction of $MgCO_3$ in dolomites can be used to infer their growth rate and the conditions required for their formation. D3 and D4 have higher degrees of order, indicating that they formed in more stable diagenetic environments with slower nucleation and crystallization rates. During their formation, the ratio of $Mg^{2+}/Ca^{2+}$was low, and often close to 1:1, resulting in a higher degree of ordering. In contrast, D1 and D2 formed in more dynamic diagenetic environments with a higher Mg^{2+}/Ca^{2+} ratio and higher concentrations of other ions in the water, leading to faster crystallization rates. As a result, the dolomite crystals formed were smaller, less crystalline, and exhibited lower ordering. Generally, dolomites from a penecontemporaneous stage tend to have lower ordering, seepage reflux dolomites have moderate ordering, and burial dolomites exhibit the highest degrees of order[10].

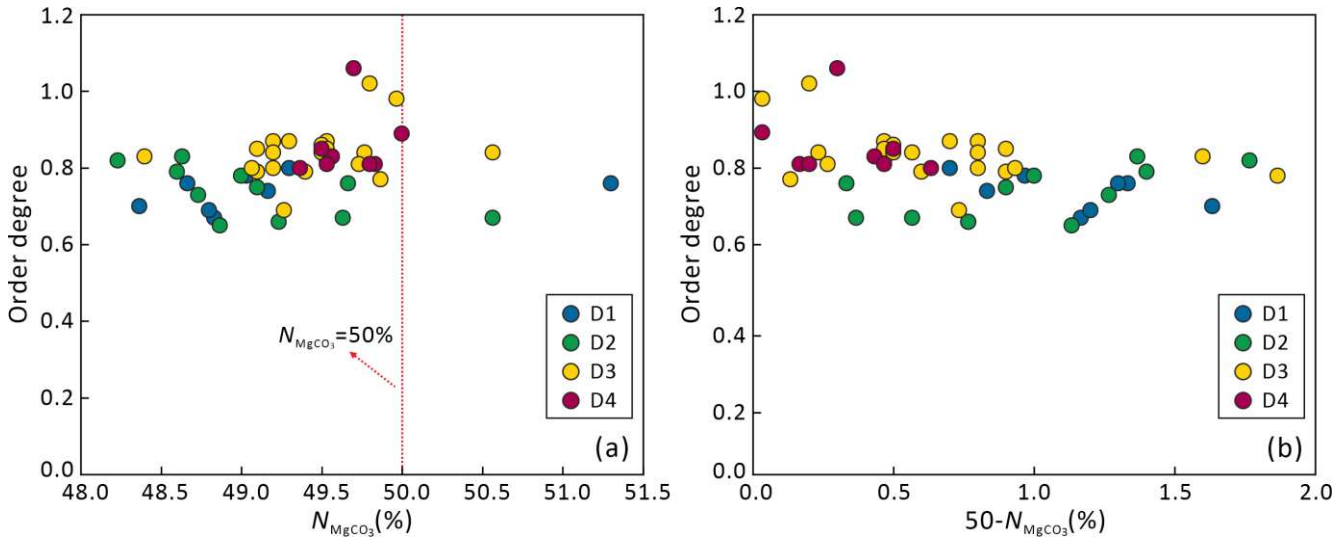


Figure 5. Relation between the order degree and the molar percentage of $MgCO_3$ in the dolomite. (a) Cross-plots of the order degree versus $N(MgCO_3)$; (b) Cross-plots of the order degree versus 50-$N(MgCO_3)$.

The coupling of crystal structure and sedimentary environment of dolomite

The dolomitization process fundamentally involves a phase transition of minerals, which inevitably alters the unit cell parameters of the mineral and consequently leads to changes in the unit cell volume[12]. The ideal dolomite has unit cell parameters of a = b = 0.48069 nm, c = 1.60034 nm, with axial angles of $\alpha = \beta = 90°$ and $\gamma = 120°$, where $MgCO_3$ and $CaCO_3$ molecular layers are alternately arranged in the lattice[44]. In the study area, the ordering degrees of the crystalline dolomites vary significantly, ranging from 0.65 to 1.06 (with an average of 0.80). The unit cell

parameter ranges between 4.795 Å and 4.806 Å (with an average of 4.802 Å) (Fig. 6a), while c ranges from 15.976 Å to 16.011 Å (with an average of 15.995 Å) (Fig. 6b). Compared to D1 and D2, the dolomites in D3 and D4 exhibit higher degrees of ordering and have unit cell parameters that are closer to those of ideal dolomite.

The correlation between Mn/Sr and Mg/Ca values in the crystalline dolomites of the XXC Formation is relatively weak (Fig. 6c). Mn is present in very low concentrations in seawater and is highly sensitive to reducing environments. The stronger the reducing environment, the more easily Mn can enter the dolomite lattice via isomorphous substitution[11]. The more intense the diagenesis experienced by dolomite, the greater the enrichment of Mn. In contrast, Sr is predominantly concentrated in seawater and tends to be progressively lost from dolomites as diagenetic intensity increases[45]. Therefore, the Mn/Sr ratio can be used as an indicator of the degree of diagenetic alteration in dolomites[46]. Specifically, Mn/Sr < 2 indicates weak diagenetic alteration; Mn/Sr values between 2 and 10 suggest moderate alteration while retaining original seawater isotopic signatures; and Mn/Sr > 10 implies intense diagenesis, where the geochemical information of dolomite has lost its interpretive value. The Mn/Sr values of the XXC Formation dolomites mostly fall between 0 and 5 (Fig. 6c), indicating that these dolomites are not of deep burial origin and still retain their original seawater isotopic signatures.

Additionally, using the paleosalinity (Z) formula proposed by Keith[47], the paleosalinity of the depositional waters was calculated (Table 2). Analyzing Z values, Mg/Ca ratios, Mn/Sr values, and unit cell parameters (a/c) as indicators of depositional environments, the results show that as salinity increases and humidity decreases, the a/c value of dolomite crystal structures tends to shift negatively (Fig. 6d). Conversely, when salinity decreases and humidity increases, the a/c value shifts positively. Furthermore, the Mg/Ca values of the crystalline dolomites are approximately 1 (Fig. 6e), indicating a high degree of dolomitization. Dolomites formed in diagenetic fluids with higher Mg/Ca ratios tend to have relatively smaller a/c values. Preliminary analysis suggests that in arid, high-salinity environments, the enrichment of not only Mg^{2+} but also larger trace elements like Mn^{2+} and Sr^{2+} leads to a significant increase in the c parameter, resulting in a negative shift in the a/c value (Fig. 6f). In contrast, in humid, low-salinity environments, the reduced Mg^{2+} content leads to a positive shift in the a/c value. However, whether the unit cell parameters trend closer to ideal dolomite still depends on the degree of recrystallization or the type of dolomitization experienced during burial.

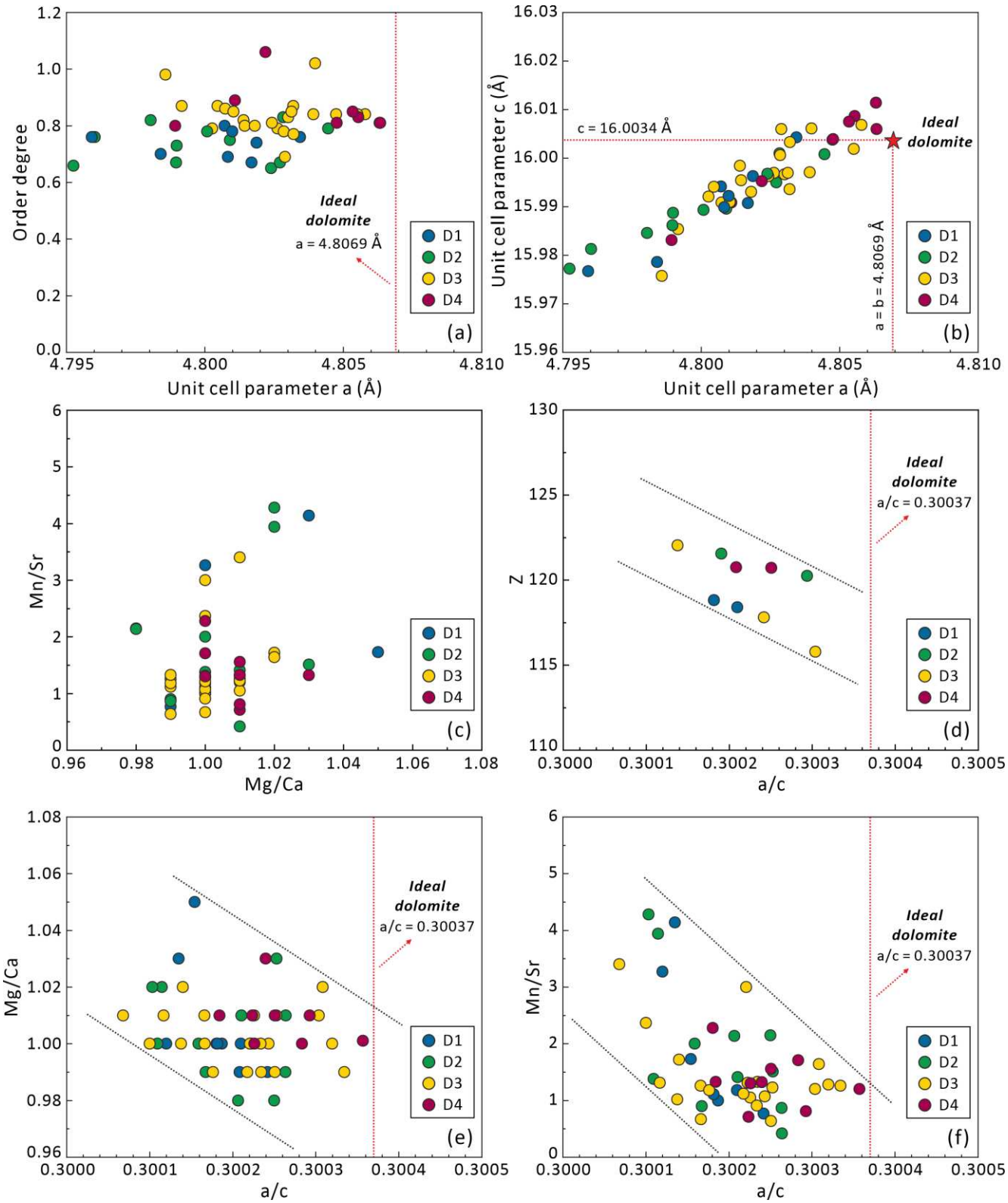


Figure 6. Interaction diagram of crystal structure and geochemical characteristics of dolomite. (a) The correlation between the degree of order and the unit cell parameters a; (b) Interaction diagram of unit cell parameters a and c; (c) Cross-plots of Mn/Sr versus Mg/Ca; (d) Cross-plots of Z versus a/c; (e) Cross-plots of Mg/Ca versus a/c; (f) Cross-plots of Mn/Sr versus a/c.

Thermal–burial history and clumped-isotope reordering modeling

Formation temperature of dolomite

Based on the formation temperature and paleogeothermal evolution of dolomite, it is possible to determine the formation depth of dolomite, which in turn aids in analyzing its genetic mechanisms. Currently, methods for determining dolomite formation temperature include oxygen isotope paleothermometry[48], fluid inclusion homogenization temperature[49], and clumped isotope thermometry[15, 18]. Unlike traditional methods, clumped isotope thermometry for carbonates is a novel technique that allows for the reconstruction of the $\delta^{18}O$ value of coeval fluids without considering the source of the parent fluid of precipitated minerals. Moreover, this method provides more accurate diagenetic temperature information.

The calibration of Bonifacie[35] was used for discussion herein based on (1) it is derived using similar analytical conditions (e.g., 90 °C acid digestion temperature) to those used in this study, and (2) although many Δ47-T calibrations had been proposed for carbonate minerals[37, 38, 50], only those proposed by Bonifacie[35], Müller[36] and Winkelstern[51] are dolomite specific. (3) It has the minor calculated $T_{\Delta 47}$ differences with that obtained by using the calibrations of Anderson[38] (Fig. 2). The formation temperatures ($T_{\Delta 47}$) of the Cambrian XXC Formation dolomites, calibrated using Δ_{47} and the temperature calibration equations, show a relatively wide distribution (Table 2). Based on the empirical formula proposed by Bonifacie[35], the formation temperatures of D1 range from 118.6 °C to 122.5 °C, D2 from 137.7 °C to 140.0 °C, D3 between 132.1 °C and 154.1 °C, and D4 from 174.9 °C to 184.6 °C. According to previous research, the seawater temperature during the deposition of the XXC Formation in the Cambrian remained relatively stable, with a paleoseawater temperature of approximately 21.2°C[8]. Assuming a geothermal gradient of 3 °C/100 m, the estimated formation depth of the dolomites in the study area is between 3247 and 5447 m. However, this depth estimation differs significantly from the petrological analysis results of the dolomites (Fig. 3).

In fact, the $T_{\Delta 47}$ obtained directly from Δ_{47} measurements in this study does not represent the true dolomitization temperature but rather the apparent equilibrium temperature[52]. The experimentally measured Δ_{47} values are negatively correlated with the calculated diagenetic temperatures (Fig. 2), indicating that the measured Δ_{47} values are likely lower than the Δ_{47} values at the time of mineral diagenesis. As a result, the $T_{\Delta 47}$ calculated from these measured values cannot accurately reflect the temperature at which the minerals underwent diagenesis. To determine the true formation temperature of the dolomites, it is necessary to restore the Δ_{47} values to those of the diagenetic period.

The effectiveness of Δ_{47} restoration of diagenetic temperature

Within a certain depth range, clumped isotope analysis of marine carbonate samples can indicate the initial surface environmental temperature. However, at greater burial depths, carbonates may undergo solid-state reordering under elevated geothermal conditions, leading to significant isotopic fractionation of Δ_{47}. This causes the $T_{\Delta 47}$ value closer to the geothermal temperatures, affecting paleotemperature reconstructions. Therefore, this study utilized stratigraphic thermal evolution histories and a solid-state reordering model to simulate the initial formation temperatures of dolomites and restore the properties of the dolomitizing fluids.

Using stratigraphic comparisons and sedimentary basin fluctuation analysis methods, along with key tectonic erosion estimates and basic geological data such as residual strata thickness and geological ages from previous studies[22, 26, 53], combined with the calibration of the measured borehole temperatures, we reconstructed the burial history of the wells at the study site and selected the well GT2 well for exhibition (Fig. 7). The Cambrian strata in central Sichuan Basin generally experienced two main phases: an early phase of large-scale subsidence and a later phase of significant uplift, with the deepest burial and highest formation temperatures reached during the Late Cretaceous. Previous bond reordering kinetics models predicted that calcite Δ_{47} values could be preserved at ambient temperatures lower than 90-100℃ for tens of million years[19, 54]. In contrast, dolomite samples can resist significant reordering at temperatures as high as 120-150℃ over the same time span[55]. However, before being uplifted to the current depth of 4.5-5.5 km, the dolomites of the XXC Formation experienced high temperature up to 230 ℃ during the late deep burial process (Fig. 7). This late-stage excessive thermal exposure caused solid-state reordering of $^{13}C^{18}O^{16}O$ within the dolomite[55], leading to high $T_{\Delta47}$ values.

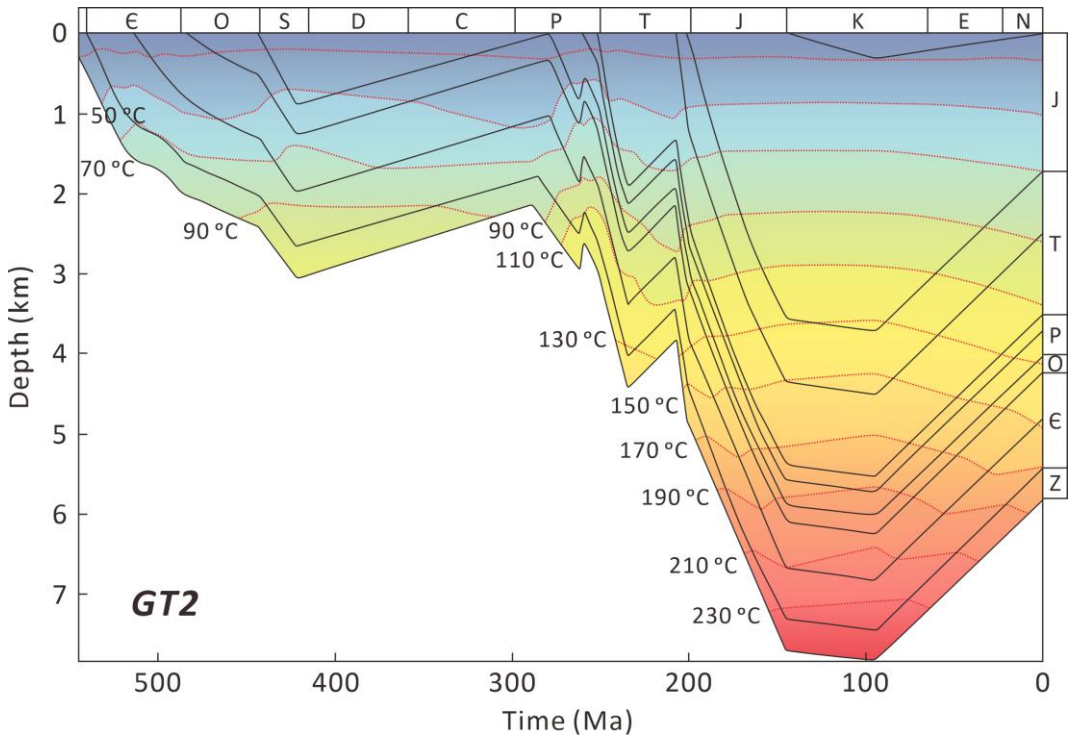


Figure 7. Burial and thermal histories evolution of Well GT2.

In the study of carbonate solid-state reordering kinetics, several reordering models have been proposed, including the transient defect/equilibrium defect model by Passey and Henkes[20], the exchange/diffusion model by Stolper and Eiler[19], and the disorder kinetics model by Hemingway and Henkes[56]. This research utilized the transient defect/equilibrium defect model (in the following the PH-Model) and the exchange/diffusion model (in the following the SE-Model) to restore the solid-state reordering evolution pathways of dolomite samples. Since clumped isotopes are highly sensitive to the maximum temperature experienced by the strata, five different theoretical T-t path models were set with maximum formation temperatures of 200 °C, 210 °C, 220 °C, 230 °C, and 240 °C, based on the burial and thermal history data of the GT2 well. The simulation results showed that the clumped isotope temperature range

of the dolomite samples (118.6-184.6 °C) closely matched the simulation results for maximum formation temperatures between 230 °C and 240 °C (Fig. 8). This indicates that the set T-t evolution paths are reasonable and accurately reflect the thermal history experienced by the samples. Thus, the maximum paleotemperature experienced by the dolomite samples of the XXC Formation is estimated to be between 230 °C and 240 °C. Using the burial history and thermal evolution data of the GT2 well, the highest paleotemperature ranges for different dolomite types, measured Δ_{47} values, and the present-day clumped isotope temperatures, various T-t evolution paths were established, and simulations were performed using both the PH and SE models.

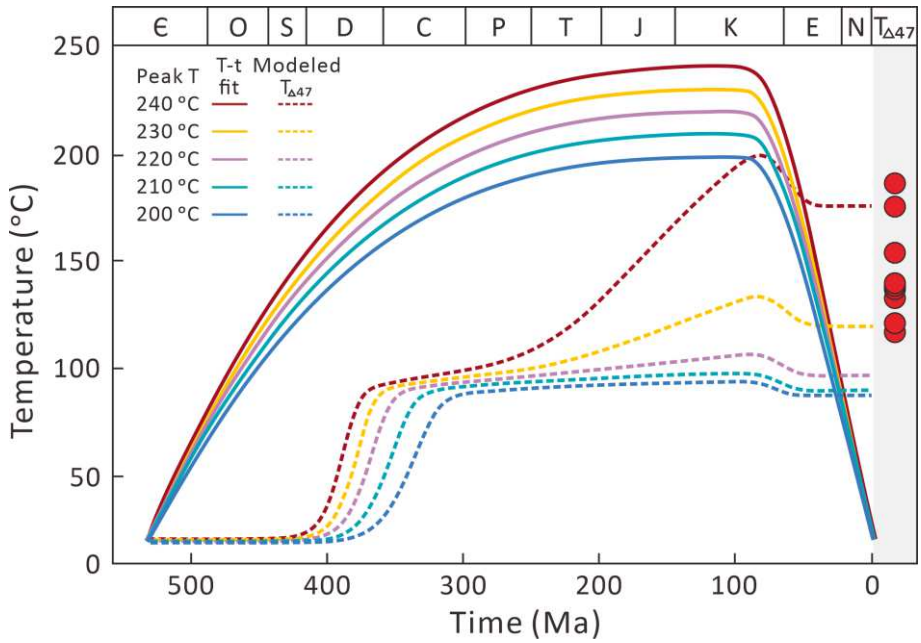


Figure 8. The highest temperature model of dolomite samples from the XXC Formation.

In the PH-Model, there were discrepancies between the measured $T_{\Delta47}$ values and the simulation results for nearly all samples (Fig. 9a). In some cases, the simulated $T_{\Delta47}$ values exceeded the formation temperature during the Cretaceous period. This is likely due to the fact that the Arrhenius parameters (E_a, K_0) for the PH-Model were derived under laboratory conditions for calcite, and it is still uncertain if they are applicable to dolomite[20]. Additionally, dolomite requires higher temperatures to initiate the ^{13}C-^{18}O bond reordering compared to calcite[57], leading to the discrepancy between measured and simulated values. Furthermore, the diagenetic environment of dolomite is more complex than calcite, and the specific timing of dolomitization is difficult to determine, introducing greater uncertainty when applying the PH-Model. Therefore, in this study, the PH-Model was unable to accurately reflect the impact of thermal history on the clumped isotope paleothermometer of dolomites in the region.

In contrast, the SE-Model is more suitable for simulating naturally evolved samples in sedimentary basins. The simulated present-day $T_{\Delta47}$ values for D1, D2, D3, and D4 range from 110.9-123.9 °C, 137.9-142.9 °C, 136.1-146.1 °C, and 174.4-178.2 °C, respectively, with no significant error compared to the measured $T_{\Delta47}$ values (Fig. 9b, Table 2). After simulation, the restored diagenetic temperature of D1 is relatively low, with a $T_{\Delta47}$ of 25.9-28.7 °C, suggesting that D1 likely formed during the contemporaneous-penecontemporaneous stage, corresponding to a diagenetic age of approximately 518.8 Ma to 516.4 Ma. The simulated diagenetic temperatures for D2 and D3 are

similar, with $T_{\Delta47}$ values of 52.8-63.4 °C and 51.5-73.3 °C, respectively, indicating formation in near-surface to shallow burial environments. Their diagenetic ages range from 510.4 Ma to 503.9 Ma for D2, and from 510.9 Ma to 475.4 Ma for D3. The restored diagenetic temperature of D4 is higher, with a $T_{\Delta47}$ of 110.5-116.2 °C, suggesting formation during the shallow to intermediate burial stage, with a corresponding diagenetic age of 251.8 Ma to 247.5 Ma. The results indicate that the SE-Model provides a more feasible forward simulation of diagenetic temperatures, with better performance in simulating solid-state reordering in the dolomites of the study area. The SE-Model demonstrates higher effectiveness in the restoration of diagenetic temperatures for the dolomites in this research.

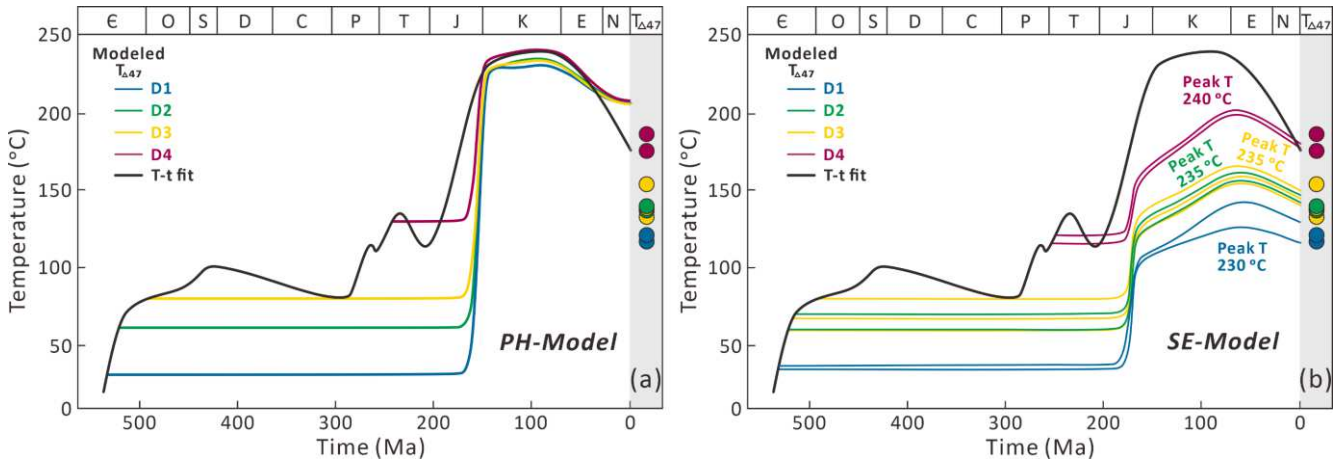


Figure 9. Diagenetic time and temperature diagrams of the dolomites of XXC Formation simulated by PH-Model (a) and SE-Model (b), respectively.

The potential effect of diagenetic alteration on initial $T_{\Delta47}$ values

By fitting the degree of ordering of various structured crystalline dolomites with their simulated initial diagenetic temperatures (Fig. 10), a strong positive correlation between dolomite ordering and crystallization temperature was observed. As the initial dolomitization temperatures of D1, D2, D3, and D4 increased, the corresponding dolomites exhibited higher degrees of ordering. This relationship is closely linked to the genetic type of dolomite, the degree of cation ordering between Mg^{2+} and Ca^{2+} in the dolomite structure, and the grain size of the dolomite crystals. The degree of cation order and crystallite size of dolomite crystals formed during geological time and under different petrogenic conditions may be related to the chemical reaction mechanism and dynamics of dolomite[58].

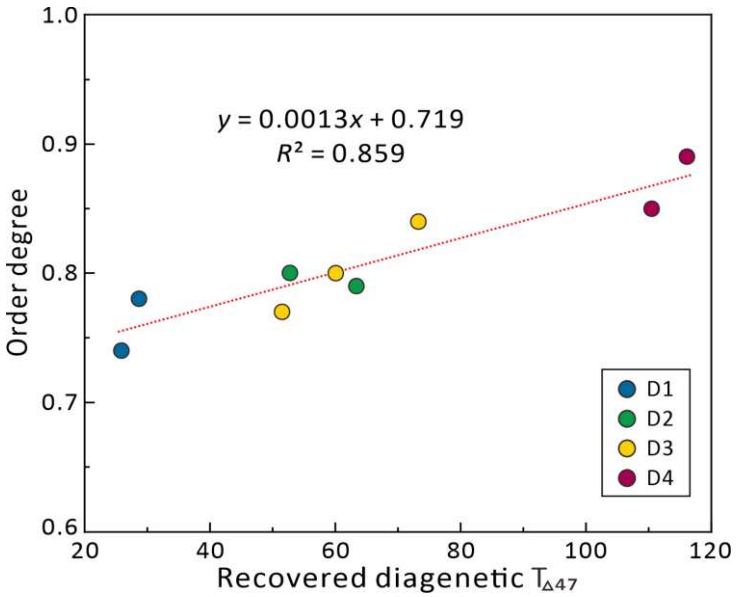


Figure 10. Relation between the order degree and initial temperatures from modeling in dolomite.

The sedimentary and diagenetic formation of dolomite can be extended over thousands to millions of years[11]. Previous studies have documented the average order degree for dolomites of ages ranging from late Precambrian to late Holocene (Fig. 11). Figure 11 shows that the lowest values of cation order mainly correspond to dolomites formed in about the last 30 Ma, and its order degree has the maximum variation. We put the order degree data of different types of crystalline dolomites in this study into Fig. 11, and find that the order degree of the dolomites formed in the Precambrian-Cambrian is obviously higher. These variations suggest a dolomite formation process extended for long periods of time during which cation order progressively increases. After relatively rapid initial dolomitization in the early stage, a subsequent increase in the cation order in the dolomite crystals might take place mainly by dissolution-recrystallization reactions extended over large geological periods of time[59, 60].

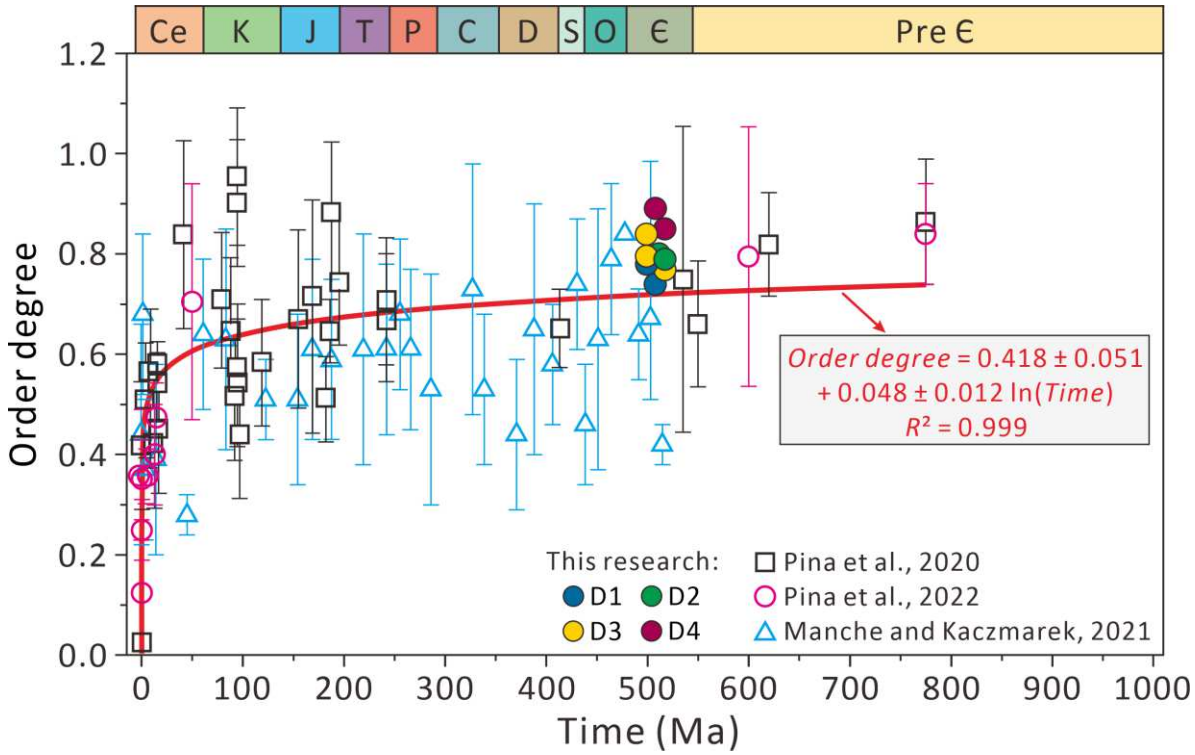


Figure 11. The order degree of dolomite versus dolomite age in million years through the late Precambrian to late Holocene (modified from[58-60]). Red line: Kell-Duivestein[61] has been fitted to all data points using the orthogonal distance regression method (Regression coefficient: $R^2 = 0.999$). Upper color bars: Ce: Cenozoic; K: Cretaceous; J: Jurassic; T: Triassic; P: Permian; C: Carboniferous; D: Devonian; S: Silurian; O: Ordovician; Є: Cambrian; Pre Є: Precambrian.

Interpretation of dolomitizing fluid and dolomitization mechanism

The variations in Sr isotopes within dolomite are an effective indicator for discerning the depositional environment and the nature of diagenetic fluids[45]. Since the residence time of Sr in seawater (approximately a million years) far exceeds the mixing time of seawater (around a thousand years), it is generally accepted that the Sr isotope composition of seawater at any given geological time is globally uniform[62]. This allows for a comparison between the Sr isotopic composition in dolomite and that of seawater, which can be used to infer the source of diagenetic fluids and the extent of external influences.

Taking into account the data resolution and regional differences, the measured $^{87}Sr/^{86}Sr$ values (0.70900-0.71000) are generally consistent with the published results of Cambrian seawater (Fig. 12). This indicates that the dolomitizing fluids were primarily marine in origin, corresponding with the same period of seawater. However, another portion of the measured $^{87}Sr/^{86}Sr$ values (ranging from 0.71000 to 0.71100) shows a significant positive deviation compared to the contemporaneous seawater (Fig. 12). This suggests that the dolomite of the XXC Formation experienced varying degrees of influence from terrestrial sources, and the diagenetic fluids may have originated from or passed through external strata enriched in radiogenic ^{87}Sr. Besides, as shown in Fig. 13a, b, the $^{87}Sr/^{86}Sr$ values have no correlation with Mn/Sr and $\delta^{18}O_{carb}$, so we can conclude that the obtained radiogenic Sr are

hydrogenous (seawater-derived).

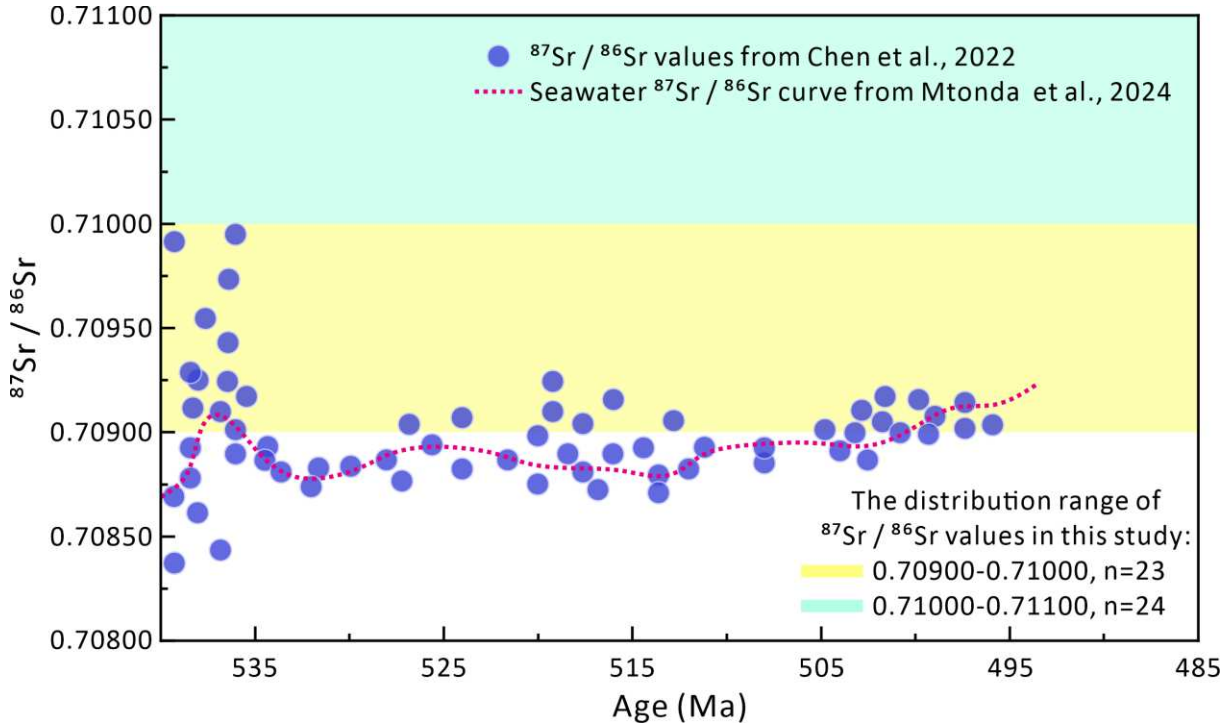


Figure 12. Distribution of $^{87}Sr/^{86}Sr$ values in dolomite of XXC Formation (modified from[45, 63]).

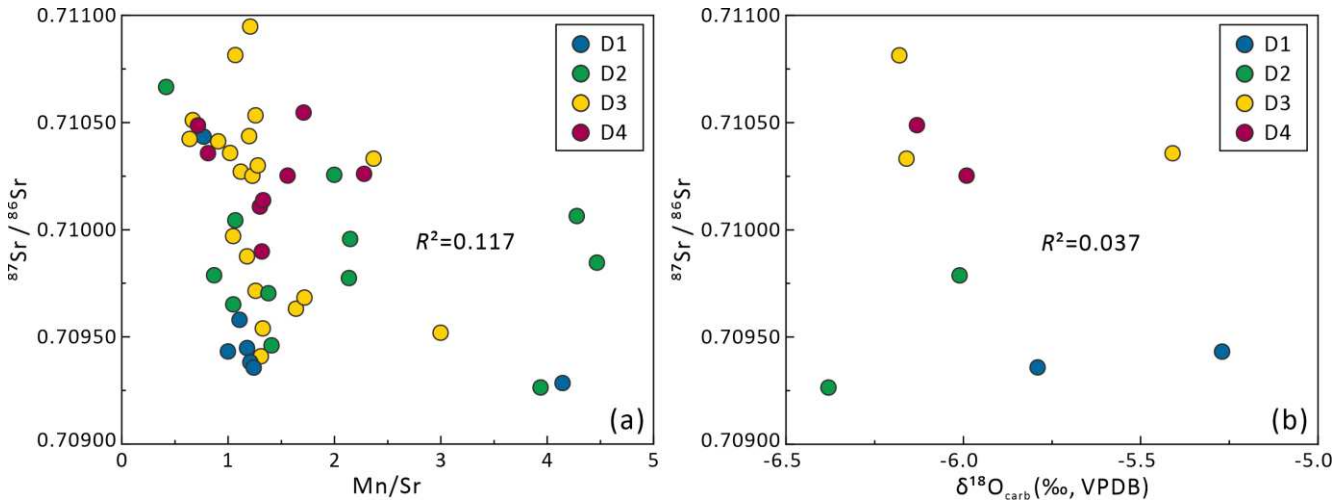


Figure 13. Correlation analysis between geochemical records. (a) $^{87}Sr/^{86}Sr$ versus Mn/Sr; (b) $^{87}Sr/^{86}Sr$ versus $\delta^{18}O_{carb}$.

The carbon and oxygen isotope compositions of seawater during the same depositional period serve as the foundational reference for understanding the variations in isotopic values in marine dolomites of different origins. By comparing the carbon and oxygen isotopic values of dolomites to those of seawater from the same depositional period, it is possible to deduce the property and source of the dolomitizing fluids, and subsequently, infer the formation environment and genesis of the dolomites. The carbon and oxygen isotopic compositions of the samples tested in this study are consistent with the stable isotopic compositions of well-preserved microfossils from the Cambrian period on a global scale (Fig. 14). The carbon and oxygen isotope values of marine cement or invertebrate

fossils generally represent the stable isotopic compositions of seawater during their formation[64, 65], making them reliable records of early Paleozoic marine environments. The $\delta^{13}C$ and $\delta^{18}O$ values of most dolomite samples from the XXC Formation fall within the distribution range of Cambrian seawater (Fig. 14). The carbon isotopic composition largely retains the characteristics of the original limestone, indicating that the dolomitizing fluids were primarily derived from contemporaneous Cambrian seawater. Furthermore, since the fractionation of carbon isotopes in dolomites is predominantly influenced by organic matter[66], a sudden enrichment of organic carbon within the dolomites could lead to the dolomitizing fluids becoming enriched in ^{12}C. This likely explains why the $\delta^{13}C$ values of a few D1 and D3 samples are significantly lower than those of Cambrian seawater (Fig. 14).

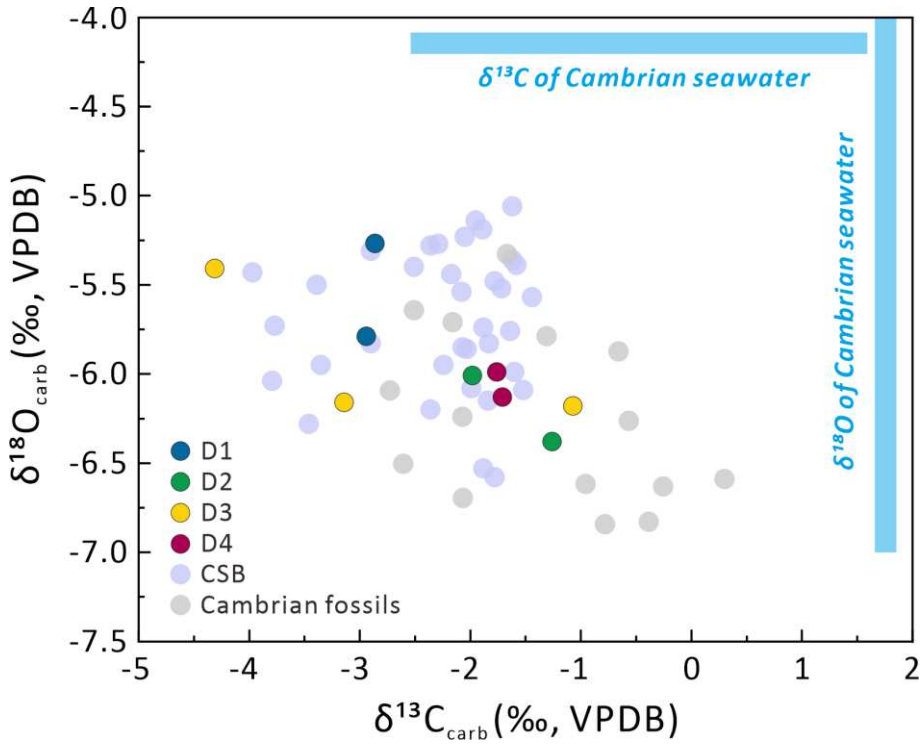


Figure 14. Cross-plots of $\delta^{18}O_{carb}$ versus $\delta^{13}C_{carb}$. Data source: The grey circle marks the range of isotopic composition of well-preserved Middle-Upper Cambrian trace fossils[67, 68]; The purple circle represents carbon and oxygen isotopes of the dolomite of XXC Formation in central Sichuan Basin (CSB) (from[8]); $\delta^{13}C$ of Cambrian seawater[64]; $\delta^{18}O$ of Cambrian seawater[65].

It is difficult to directly determine the $\delta^{18}O$ of the diagenetic fluid because the fluid in the present formation is the residual fluid after diagenesis and has been affected by the water-rock reaction[17]. Therefore, to reconstruct the dolomitizing fluid properties of the XXC Formation in the study area, we used the $10^3 \ln\alpha$-T equation from Horita[14], to constrain the $\delta^{18}O_{fluid}$ (‰; VSMOW: Vienna Standard Mean Ocean Water) using $T_{\Delta 47}$ (calculated temperature derived from Δ_{47}) and $\delta^{18}O_{dolomite}$:

$$10^3 \ln\alpha_{dolomite\text{-}fluid} = 3.14 * 10^6 * T^{-2} - 3.14 \qquad (8)$$

In Eq. (8), $\alpha_{dolomite\text{-}fluid} = (\delta^{18}O_{dolomite} + 1000) / (\delta^{18}O_{fluid} + 1000)$. The $\delta^{18}O_{dolomite}$ is in VSMOW. The $\delta^{18}O_{dolomite}$ (VPDB) is transferred into $\delta^{18}O_{dolomite}$ (VSMOW) by using[69]: $\delta^{18}O_{dolomite}$ (VSMOW) = 1.03092 * $\delta^{18}O_{dolomite}$ (VPDB) + 30.92.

We calculated $\delta^{18}O$ compositions of the diagenetic fluids ($\delta^{18}O_{fluid}$) versus paired $T_{\Delta 47}$ data（Fig. 15）, plotted on a diagram of reference values for modern carbonates and coexisting diagenetic fluids equilibrated over a range of geological conditions[70]. Suppose a ~6.5‰ depletion of ^{18}O in Cambrian seawater relative to modern seawater is taken into consideration[71], the corrected $\delta^{18}O_{fluid}$-$T_{\Delta 47}$ data favor a late diagenetic to anchimetamorphism, strongly rock-buffered environment for recrystallization (Fig. 15). Furthermore, a restricted marine/evaporite to early diagenetic, fluid-buffered environment and a late diagenetic, rock-buffered environment is indicated if we calculate corrected $\delta^{18}O_{fluid}$ values using the initial $T_{\Delta 47}$ values of our samples as derived from the SE-Model (Fig. 15). The distribution range of $\delta^{18}O_{fluid}$ values determined after recovery by solid-state reordering is large, and this deviation can be explained by the enrichment of $\delta^{18}O_{fluid}$ values in the fluid phase in response to increasing temperatures at burial[29].

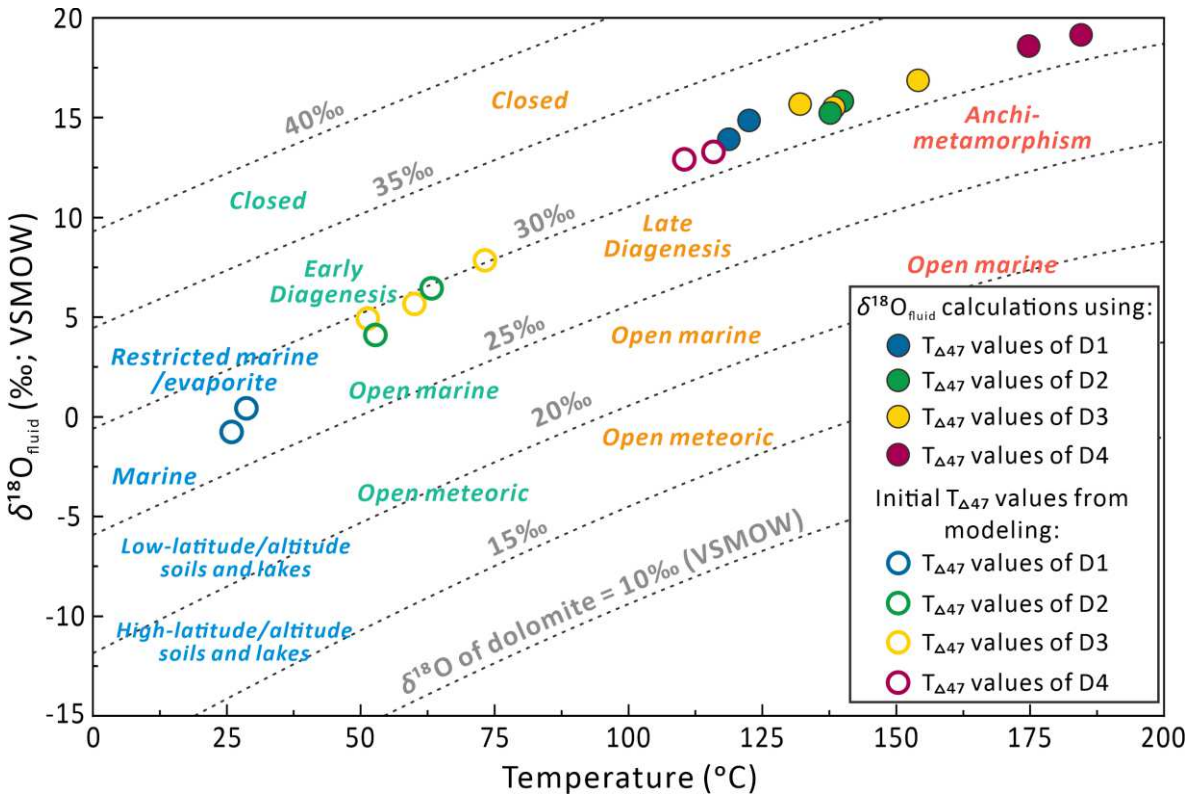


Figure 15. Clumped isotope temperatures of the dolomite samples are plotted against their fluid source $\delta^{18}O_{fluid}$. Dashed lines represent $\delta^{18}O$ of dolomite using the temperature relationship[14].

In conclusion, the diagenetic evolution of the dolomites in the XXC Formation underwent both marine and burial diagenetic processes. The $\delta^{18}O_{fluid}$ values of the parental fluids indicate a restricted marine/evaporite-late diagenetic environment, spanning a significant temporal range throughout the diagenetic evolution. During the contemporaneous-penecontemporaneous stage, the evaporation and concentration of Mg-rich seawater facilitated near-surface sabkha dolomitization of early sediments such as calcite or aragonite muds, resulting in D1 under fluid-buffered conditions. This interpretation aligns with paleo plate research, which suggests that the Sichuan Basin was situated at 30°N, 105°E during the Cambrian and that the XXC Formation in central Sichuan Basin was deposited in a warm to hot subtropical climate[8]. In the early diagenetic stage, as burial depth and temperature increased, D2,

D3 and pore waters transitioned from an open to a semi-closed to closed shallow burial environment. Recrystallization of early dolomites occurred, with dolomitizing fluids likely originating from Cambrian seawater confined within shallow burial strata rather than from surface seawater. Regarding the long-term preservation of seawater in the pores, we suggest that the preservation of these fluids may be due to the limited permeability of the overlying strata during early burial stages, which could have effectively sealed the pore spaces. This sealing may have allowed residual seawater to persist, thus facilitating the dolomitization process. Additionally, the relatively low temperatures and pressures during the early stages of burial might have slowed down the exchange of pore fluids, allowing for the preservation of seawater. During the late diagenetic stage, D4 in the middle burial environment were largely removed from oxidizing conditions. As burial depth, temperature, and pressure increased, acidic formation fluids (e.g., CO_2 and organic acids) enhanced reservoir properties by creating dissolution pores and fractures (Fig. 3j, l). The initially disordered dolomite deposited in seawater or pore water gradually transformed into ordered dolomite during the early to late diagenetic evolution (Fig. 10; Fig. 11).

Conclusion

Although the crystal structure of different types of crystalline dolomites exhibits varying responses to the environment, their C-O-Sr isotope analyses indicate that the dolomitizing fluid was primarily associated with contemporaneous Cambrian seawater. Crucially, the degree of cation ordering in D1-D4 shows a strong positive correlation with their simulated initial diagenetic temperatures, indicating that, over extensive geological periods, dissolution-recrystallization reactions have led to changes in dolomite crystal lattice volume. As a result, the crystal structure becoming increasingly ordered, with the lattice parameters approaching those of ideal dolomite.

The Cambrian XXC Formation dolomites preserve a unique record of marine diagenesis modulated by burial thermal history. The Δ_{47} evolution of the crystalline dolomites was predicted with the exchange/diffusion model, constrained by independent thermal history reconstruction and Δ_{47} values. This approach excludes the effects of dolomite solid-state reordering under high temperature (~230°C) deep burial conditions.

Clumped isotope can be an effective technique for determining the $\delta^{18}O$ of the dolomitization fluid, the $\delta^{18}O_{fluid}$ values of the parental fluid point to a restricted marine/evaporitic-late diagenetic environment. The diagenetic stages include the contemporaneous-penecontemporaneous stage, early diagenesis, and late diagenesis, where initially disordered dolomite deposited in seawater or porewater gradually became more ordered through early to late diagenetic evolution.

Data availability

The authors confirm that the data supporting the findings of this study are available within the article.

Acknowledgements

This study is funded by the National Natural Science Foundation of China (grant no. 42002178). We acknowledge

this generous funding from the China National Petroleum Corporation.

Author contributions

Jiakai Hou and Guangyou Zhu designed the research ideas experimental methods, discussed the results and implications, and commented on the manuscript at all stages. Hongbin Li performed the experiments. Lizhen Wang compiled geological maps. All authors reviewed the manuscript.

Declaration of Competing Interest

The authors declare that they have no known competing financial interests or personal relationships that could have appeared to influence the work reported in this paper.

References

1. Hardie, L.A., 1987. Dolomitization; a critical view of some current views. Journal of Sedimentary Research, 57(1): 166-183.
2. Land, L.S., 1998. Failure to precipitate dolomite at 25 °C from dilute solution despite 1000-fold oversaturation after 32 years. Aquatic Geochemistry, 4(3): 361-368.
3. Dennis, K.J., Schrag, D.P., 2010. Clumped isotope thermometry of carbonatites as an indicator of diagenetic alteration. Geochimica et Cosmochimica Acta, 74(14): 4110-4122.
4. Zhao, W.Z., Shen, A.J., Qiao, Z.F., Pan, L.Y, Hu, A.P., Zhang, J., 2018b. Genetic types and distinguished characteristics of dolomite and the origin of dolomite reservoirs. Petroleum Exploration and Development, 45(6): 983-997.
5. Liu, H., Tan, X.C., Li, L., Luo, B., Ma, C.L., Yang, L.G., 2011. Characteristics and main controlling factors of porous carbonate reservoirs : A case from the Jia 5 Member of the Jialingjiang Formation , southwest Sichuan Basin. Petroleum Exploration and Development, 38(03): 275-281.
6. Luo, C.Y., Spread, S., Wang, X.Z., Liu, Y., Zeng, D.M., Li, J.L., 2009. The influence of constituent rock action on reservoir in Feixianguan area of northeast Sichuan Province. Journal of Oil and Gas Technology, 31(05): 182-189.
7. Ding, X., Tan, X.C., Zhou, Y., Chen, J.S., Tang, Q.S., Hu, W.W., 2012. Reservoir characteristics and genesis of the second member of Jia Formation in central Sichuan Basin. Journal of Chengdu University of Technology (in Chinese), 39(03): 269-276.
8. Li, X., Zhu, G.Y., Li, T.T., Zhou, L., Wu, Y.X., Tian, L.J., 2022. Mg isotope characteristics and genetic mechanism of dolomite of Cambrian Xixiangchi Formation in central Sichuan. Acta Petrolei Sinica (in Chinese), 43(11): 1585-1603.
9. Friedman, G.M., 2007. Structurally controlled hydrothermal dolomite reservoir facies: An overview: Discussion. AAPG Bulletin, 91(9): 1339-1341.
10. Zhu, G.Y., Li, X., 2023a. Advances in genetic types and research methods of dolomites. Acta Petrolei Sinica, 44(07): 1167-1190.
11. Warren, J., 2000. Dolomite: occurrence, evolution and economically important associations. Earth-Science Reviews, 52(1): 1-81.
12. Zhu, G.Y., Wei, Z.L., Wu, X.Y., Li, Y.B., 2023b. New insights into the dolomitization and dissolution mechanisms of dolomite-calcite (104)/(110) crystal boundary: An implication to geologic carbon sequestration process. Science of The Total Environment, 904: 166273.
13. Vasconcelos, C., McKenzie, J.A., Warthmann, R., Bernasconi, S.M., 2005. Calibration of the δ18O paleothermometer for dolomite precipitated in microbial cultures and natural environments. Geology, 33(4): 317-320.
14. Horita, J., 2014. Oxygen and carbon isotope fractionation in the system dolomite–water–CO_2 to elevated temperatures. Geochimica et Cosmochimica Acta, 129: 111-124.
15. Chang, B., Li, C., Liu, D., Foster, I., Tripati, A., Lloyd, M.K., Maradiaga, I., Luo, G., An, Z.H., She, Z.B., Xie, S.C., Tong, J.N., Huang, J.H., Algeo, T.J., Lyons, T.W., Immenhauser, A., 2020. Massive formation of early diagenetic dolomite in the Ediacaran ocean: Constraints on the “dolomite problem”. Proceedings of the National Academy of Sciences, 117: 14005-14014.
16. Hu, X.L., Müller, I.A., Zhao, A.k., Ziegler, M., Chen, Q., Han, L., Shi, Z.Q., 2022. Clumped isotope thermometry reveals diagenetic origin of the dolomite layer within late Ordovician black shale of the Guanyinqiao Bed (SW China). Chemical Geology, 588: 120641.
17. Li, P.P., Zou, H.Y., Hao, F., Yu, X.Y., Wang, G.W., Eiler, J.M., 2020. Using clumped isotopes to determine the origin of the Middle Permian Qixia Formation dolostone, NW Sichuan Basin, China. Marine and Petroleum Geology, 122: 104660.
18. Muñoz-López, D., Lu, C.J., Li, W.Q., Corlett, H., Hollis, C., Swart, P.K., Koeshidayatullah, A., 2024. What is the source of magnesium in hydrothermal

dolomites? New insights from coupling δ26Mg - Δ47 isotopes. Earth and Planetary Science Letters, 638: 118760.
19. Stolper, D.A., Eiler, J.M., 2015. The kinetics of solid-state isotope-exchange reactions for clumped isotopes: A study of inorganic calcites and apatites from natural and experimental samples. American Journal of Science, 315: 363-411.
20. Passey, B., Henkes, G., 2012. Carbonate clumped isotope bond reordering and geospeedometry. Earth and Planetary Science Letters, 223–236.
21. Yang, X.F., Huang, Z.S., Wang, X.Z., Wang, Y.P., Li, K., Zeng, D.M., 2019. Origin of crystal dolomite and its reservoir formation mechanism in the Xixiangchi Formation, Upper Cambrian in Southeastern Sichuan basin. Carbonates and Evaporites, 34(4): 1537-1549.
22. Shi, S.Y, Wang, T.S., Liu, W., Jiang, H., Li, Q.F., Liu, X., Zeng, Y.Y., Zou X., Hu L., 2020. Reservoir characteristics and natural gas exploration potential of the Cambrian Xixiangchi Formation in Sichuan Basin. Natural Gas Geoscience, 31(06): 773-785.
23. Zhang, T., Li, Y.F., Fan, T.L, Silva, A.C.D., Kuang, M.Z., Liu, W.W, Ma, C., Gao, Q., Shi, J.Y., Gao, Z.Q., Li, M.S., 2022. Orbital forcing of tropical climate dynamics in the Early Cambrian. Global and Planetary Change, 219: 103985.
24. Zhang, S.C., Wang, H.J., Su, J., Wang, X.M., He, K., Liu, Y.K., 2024. Control of Earth system evolution on the formation and enrichment of marine ultra-deep petroleum in China. Petroleum Exploration and Development, 51(4): 870-885.
25. Zhao, G.C., Wang, Y.J., Huang, B.C., Dong, Y.P, Li, S.Z., Zhang, G.W., Yu, S., 2018a. Geological reconstructions of the East Asian blocks: From the breakup of Rodinia to the assembly of Pangea. Earth-Science Reviews, 186: 262-286.
26. Liu, X., Qiu, N.S., Feng, G.G., Song, J.L., Li, C.J., 2023. Thermal evolution of Permian system in eastern Sichuan under isotopic constraints of carbonate clusters. Acta Geologica Sinica (in Chinese), 97(08): 2676-2689.
27. Du, J.H., Zou, C.N., Xu, C.C., He, H.Q., Shen, P., Yang, Y.M., Li, Y.L., Wei, G.Q., Wang, Z.C., Yang, Y., 2014. Theoretical and technical innovations in strategic discovery of a giant gas field in Cambrian Longwangmiao Formation of central Sichuan paleo-uplift, Sichuan Basin. Petroleum Exploration and Development, 41(3): 294-305.
28. Zou, C.N., Du, J.H., Xu, C.C., Wang, Z.C., Zhang, B.M., Wei, G.Q., Wang, T.S., Yao, G.S., Deng, S.H., Liu, J.J., Zhou, H., Xu, A., Yang, Z., Jiang, H., Gu, Z.D., 2014. Formation, distribution, resource potential, and discovery of Sinian–Cambrian giant gas field, Sichuan Basin, SW China. Petroleum Exploration and Development, 41(3): 306-325.
29. Liang, J.T., Azmy, K., Liu, K.Y., Liu, S.B., Li, L.P., Zhou, G., Qiu, Y.C., Li, W.Z., He, Y., Wen, H.G., 2023. Petrographic and geochemical characteristics of the Middle−Upper Cambrian Xixiangchi dolomites in the central Sichuan Basin, southwest China: Implications for dolomite origins and dolomitization mechanisms. Marine and Petroleum Geology, 152: 106215.
30. Wei, G.Q., Yang, W., Du, J.H., Xu, C.C., Zou, C.N., Xie, W.R, Wu, S.J., Zeng, F.Y., 2015. Tectonic features of Gaoshiti-Moxi paleo-uplift and its controls on the formation of a giant gas field, Sichuan Basin, SW China. Petroleum Exploration and Development, 42(3): 283-292.
31. Zhu, G.Y., Zhang, Z.Y., Jiang, H., Yan, L., Chen, W.Y., Li, T.T., Li, X., 2023c. Evolution of the Cryogenian cratonic basins in China, paleo-oceanic environment and hydrocarbon generation mechanism of ancient source rocks, and exploration potential in 10,000 m-deep strata. Earth-Science Reviews, 244: 104506.
32. Dennis, K.J., Affek, H.P., Passey, B.H., Schrag, D.P., Eiler, J.M., 2011. Defining an absolute reference frame for 'clumped' isotope studies of CO_2. Geochimica et Cosmochimica Acta, 75(22): 7117-7131.
33. Eiler, J.M., 2007. "Clumped-isotope" geochemistry—The study of naturally-occurring, multiply-substituted isotopologues. Earth and Planetary Science Letters, 262(3): 309-327.
34. Wang, R., Xiao, Y., Yu, K.F., Jones, B., Wu, L., Liang, F., Yang Y., Chang B., 2022. Temperature regimes during formation of Miocene island dolostones as determined by clumped isotope thermometry: Xisha Islands, South China Sea. Sedimentary Geology, 429: 106079.
35. Bonifacie, M., Calmels, D., Eiler, J.M., Horita, J., Chaduteau, C., Vasconcelos, C., Agrinier, P., Katz, A., Passey, B.H., Ferry, J.M., Bourrand, J.J., 2017. Calibration of the dolomite clumped isotope thermometer from 25 to 350°C, and implications for a universal calibration for all (Ca, Mg, Fe)CO_3 carbonates. Geochimica et Cosmochimica Acta, 200: 255-279.
36. Müller, I.A., Rodriguez-Blanco, J.D., Storck, J.C., Nascimento, G.S.D., Bontognali, T.R.R., Vasconcelos, C., Benning, L.G., Bernasconi, S.M., 2019. Calibration of the oxygen and clumped isotope thermometers for (proto-)dolomite based on synthetic and natural carbonates. Chemical Geology, 525: 1-17.
37. Petersen, S.V., Defliese, W.F., Saenger, C., Daëron, M., Huntington, K.W., John, C.M., Kelson, J.R., Bernasconi, S.M., Colman, A.S., Kluge, T., Olack, G.A., Schauer, A.J., Bajnai, D., Bonifacie, M., Breitenbach, S.F.M., Fiebig, J., Fernandez, A.B., Henkes, G.A., Hodell, D., Katz, A., Kele, S., Lohmann, K.C., Passey, B.H., Peral, M.Y., Petrizzo, D.A., Rosenheim, B.E., Tripati, A., Venturelli, R., Young, E.D., Winkelstern, I.Z., 2019. Effects of Improved 17O Correction on Interlaboratory Agreement in Clumped Isotope Calibrations, Estimates of Mineral-Specific Offsets, and Temperature Dependence of Acid Digestion Fractionation. Geochemistry, Geophysics, Geosystems, 20(7): 3495-3519.
38. Anderson, N.T., Kelson, J.R., Kele, S., Daëron, M., Bonifacie, M., Horita, J., Mackey, T.J., John, C.M., Kluge, T., Petschnig, P., Jost, A.B., Huntington, K.W., Bernasconi, S.M., Bergmann, K.D., 2021. A Unified Clumped Isotope Thermometer Calibration (0.5-1,100°C) Using Carbonate-Based Standardization. Geophysical Research Letters, 48(7): e2020GL092069.
39. Sibley, D.F., Gregg, J.M., 1987. Classification of dolomite rock textures. Journal of Sedimentary Research, 57(6): 967-975.
40. Füchtbauer, H., 1974. Sediments and sedimentary rocks 1. Part II of sedimentary petrology. Geological Magazine, 113(01): 86-87.
41. Zeng, L., Wan, M.X., Peng, Y., 2004. Order degree of dolomite and its application in petroleum geology. Natural Gas Exploration and Development (04):

64-85.
42. Hu, J.J., Li, Q., Chen, R.Y., Shao, W., Ge, D.S., Huang, J., 2014. Study on controlling factors of order degree of dolomite in middle and Lower Permian carbonate rocks in Qiangtang Basin. Journal of Mineralogy and Petrology (in Chinese), 34(02): 91-95.
43. Land, L.S., 1985. The origin of massive dolomite. Journal of Geological Education, 33: 112-125.
44. Li, X., Zhu, G.Y., Zhang, Z.Y., 2024. Genesis of ultra-deep dolostone and controlling factors of large-scale reservoir: A case study of the Sinian Dengying Formation and the Cambrian Longwangmiao Formation in the Sichuan Basin. Science China Earth Sciences, 67(7): 2352-2382.
45. Chen, X., Zhou, Y., Shields, G.A., 2022. Progress towards an improved Precambrian seawater $^{87}Sr/^{86}Sr$ curve. Earth-Science Reviews, 224: 103869.
46. Kaufman, A.J., Jacobsen, S.B., Knoll, A.H., 1993. The Vendian record of Sr and C isotopic variations in seawater: Implications for tectonics and paleoclimate. Earth and Planetary Science Letters, 120(3): 409-430.
47. Keith, M.L., Weber, J.N., 1964. Carbon and oxygen isotopic composition of selected limestones and fossils. Geochimica et Cosmochimica Acta, 28(10): 1787-1816.
48. Kaufman, J., Hanson, G.N., Meyers, W.J., 1991. Dolomitization of the Devonian Swan Hills Formation, Rosevear Field, Alberta, Canada. Sedimentology, 38: 41-66.
49. Wang, G., Li, P., Hao, F., Zou, H., Yu, X., 2015. Origin of dolomite in the third member of Feixianguan Formation (Lower Triassic) in the Jiannan area, Sichuan Basin, China. Marine and Petroleum Geology, 63: 127-141.
50. Zaarur, S., Affek, H.P., Brandon, M.T., 2013. A revised calibration of the clumped isotope thermometer. Earth and Planetary Science Letters, 382: 47-57.
51. Winkelstern, I.Z., Kaczmarek, S.E., Lohmann, K.C., Humphrey, J.D., 2016. Calibration of dolomite clumped isotope thermometry. Chemical Geology, 443: 32-38.
52. Li, P.P., Wang, C., Zou, H.Y., Yu, X.Y., 2021. Application and limitation of cluster isotopes in dolomitization fluid recovery. Oil & Gas Geology (in Chinese), 42(03): 738-746.
53. Deng, B., Liu, S.G., Liu, S., Li, Z.W., Zhao, J.C., 2009. Restoration of surface denudation in Sichuan Basin and its significance. Journal of Chengdu University of Technology (in Chinese), 36(06): 675-686.
54. Henkes, G.A. Passey, B.H., Grossman, E.L., Shenton, B.J., Pérez-Huerta, A., Yancey, T.E., 2014. Temperature limits for preservation of primary calcite clumped isotope paleotemperatures. Geochimica et Cosmochimica Acta, 139: 362-382.
55. Lloyd, M.K., Ryb, U., Eiler, J.M., 2018. Experimental calibration of clumped isotope reordering in dolomite. Geochimica et Cosmochimica Acta, 242: 1-20.
56. Hemingway, J.D., Henkes, G.A., 2021. A disordered kinetic model for clumped isotope bond reordering in carbonates. Earth and Planetary Science Letters, 566: 116962.
57. Bonifacie, M., Calmels, D., Eiler, J., 2013. Clumped isotope thermometry of marbles as an idicator of the closure temperatures of calcite and dolomite with respect to solid-state reordering of C–O bonds. Mineralogical Magazine, 77(5): 735.
58. Pina, C.M., Pimentel, C., Crespo, Á., 2022. The Dolomite Problem: A Matter of Time. ACS Earth and Space Chemistry, 6(6): 1468-1471.
59. Pina, C.M., Pimentel, C., Crespo, Á., 2020. Dolomite cation order in the geological record. Chemical Geology, 547: 119667.
60. Manche, C.J., Kaczmarek, S.E., 2021. A global study of dolomite stoichiometry and cation ordering through the Phanerozoic. Journal of Sedimentary Research, 91(5): 520-546.
61. Kell-Duivestein, I.J., Baldermann, A., Mavromatis, V., Dietzel, M., 2019. Controls of temperature, alkalinity and calcium carbonate reactant on the evolution of dolomite and magnesite stoichiometry and dolomite cation ordering degree - An experimental approach. Chemical Geology, 529: 119292.
62. Veizer, J., Compston, W., 1974. 87Sr/86Sr composition of seawater during the Phanerozoic. Geochimica et Cosmochimica Acta, 38(9): 1461-1484.
63. Mtonda, M.T., Le, R.P., Taylor, W.L., Wilton, A., Tostevin, R., 2024. High resolution strontium isotope data from Nama Group, South Africa, constrain global stratigraphic relationships in the terminal Ediacaran. Precambrian Research, 404: 107339.
64. Montañez, I., Osleger, D., Banner, J., Mack, M., 2000. Evolution of the Sr and C isotope composition of Cambrian Oceans. GSA Today, 10: 1-5.
65. Veizer, J., Ala, D., Azmy, K., Bruckschen, P., Buhl, D., Bruhn, F., Carden, G.A.F., Diener, A., Ebneth, S., Godderis, Y., Jasper, T., Korte, C., Pawellek, F., Podlaha, O.G., Strauss, H., 1999. 87Sr/86Sr, δ13C and δ18O evolution of Phanerozoic seawater. Chemical Geology, 161: 59-88.
66. Kennedy, M.J., 1996. Stratigraphy, sedimentology, and isotopic geochemistry of Australian Neoproterozoic postglacial cap dolostones; deglaciation, delta ^{13}C excursions, and carbonate precipitation. Journal of Sedimentary Research, 66(6): 1050-1064.
67. Azizi, A., Bakhouch, A.E., Albani, A.E., Kirsimäe, K., Halim, M.E., Hariri, K.E., Erragragui, M., Hafid, A., Vinn, O., 2023. First record of trace fossils in the Ediacaran–Cambrian transition on the northern Gondwana platform (Anti-Atlas, Morocco). Precambrian Research, 399: 107227.
68. Brasier, M., Cowie, J., Taylor, M., 1994. Decision on the Precambrian-Cambrian boundary stratotype. Episodes, 17(1): 3-8.
69. Kim, S.T., Coplen, T.B., Horita, J., 2015. Normalization of stable isotope data for carbonate minerals: Implementation of IUPAC guidelines. Geochimica et Cosmochimica Acta, 158: 276-289.
70. Eiler, J.M., 2011. Paleoclimate reconstruction using carbonate clumped isotope thermometry. Quaternary Science Reviews, 30(25): 3575-3588.
71. Jaffrés, J.B.D., Shields, G.A., Wallmann, K., 2007. The oxygen isotope evolution of seawater: A critical review of a long-standing controversy and an improved geological water cycle model for the past 3.4 billion years. Earth-Science Reviews, 83(1): 83-122.